

Supporting Information For:

Dual-Responsive Zr(IV) MOF Based Fluorometric Sensor for Rapid and Selective Detection of Anti-Cancer Drug Dacarbazine and Herbicide Oryzalin in Environmental and Biological Samples

Paltan Laha,^a Subhrajyoti Ghosh,^a Mostakim SK^b and Shyam Biswas^{a}*

^a Department of Chemistry, Indian Institute of Technology Guwahati, 781039, Assam, India.

^b Department of Chemical Science, Indian Institute of Science Education and Research Berhampur, Main Campus, 760003, India.

*Corresponding author. Tel: 91-3612583309

E-mail address: sbiswas@iitg.ac.in

Materials and Characterization Methods:

All of the chemicals were purchased from commercial suppliers and used directly without further purification. The 2-(benzofuran-2-carboxamido) terephthalic acid (H₂L) was prepared according to the below mentioned procedure. The Attenuated Total Reflectance Infrared (ATR-IR) spectra were recorded using PerkinElmer UATR Two at the ambient condition in the region 400-4000 cm⁻¹. The notations used for characterization of the bands are broad (br), strong (s), very strong (vs), medium (m), weak (w) and shoulder (sh). Fluorescence sensing studies were performed with a HORIBA JOBIN YVON Fluoromax-4 spectrofluorometer. Fluorescence lifetimes were measured using Picosecond Time-resolved and Steady State Luminescence Spectrometer on an Edinburg Instruments Lifespec II & FSP 920 instrument. A Bruker Avance III 600 NMR spectrometer was used for recording ¹H and ¹³C NMR spectra at 500 MHz. The mass spectrometry of the synthesized linker was obtained with Ultra-High Performance Liquid Chromatograph - Quadrupole Time of Flight - High Resolution Mass Spectrometer (UHPLC-QTOF-HRMS, Agilent G6546A). Thermogravimetric analysis (TGA) was carried out with a Netzsch STA-409CD thermal analyzer in the temperature range of 30-700 °C in an O₂ atmosphere at the heating rate of 4 °C min⁻¹. PXRD data were collected by using Rigaku Smartlab X-ray diffractometer with Cu-K α radiation ($\lambda = 1.54056 \text{ \AA}$), 40 kV of operating voltage and 125 mA of operating current. N₂ sorption isotherms were recorded by using Quantachrome Quadrasorb evo volumetric gas adsorption equipment at -196 °C. Before the sorption analysis, the degassing of the compound was carried out at 100 °C under a high vacuum for 24 h. Gemini 500 was utilized for Energy Dispersive X-rays spectrometer (EDX) for elemental characterization. FE-SEM images were captured with a Zeiss (SIGMA 300) scanning electron microscope. FE-TEM image was captured with a JEOL Field Emission - Transmission electron microscope. Pawley refinement was carried out using Materials Studio software.

Fluorescence Detection of DCZ in Human Blood Serum Samples:

From the right arm vein of a completely healthy individual (blood group: O⁺), 10 mL of blood sample was taken out and centrifuged at 12000 rpm for 20 min to separate out the blood plasma. The pale-yellow coloured blood serum was collected in a Falcon tube and kept in a refrigerator at -20 °C. For fluorescence detection experiments, aliquots of different concentrations of DCZ were spiked into the human blood serum sample, which contained HEPES buffer suspension of the probe.

Fluorescence Detection of DCZ in Human Urine Samples:

From a completely healthy individual, 10 mL of first early morning urine sample was collected and 500 μ L of HNO₃ was poured into the sample to eliminate all the interfering living organisms. The sample was centrifuged at 10000 rpm for 15 min. The supernatants were taken for the experiments. For fluorescence detection experiments, different aliquots of DCZ were spiked in the urine sample containing HEPES buffer suspension of the probe.

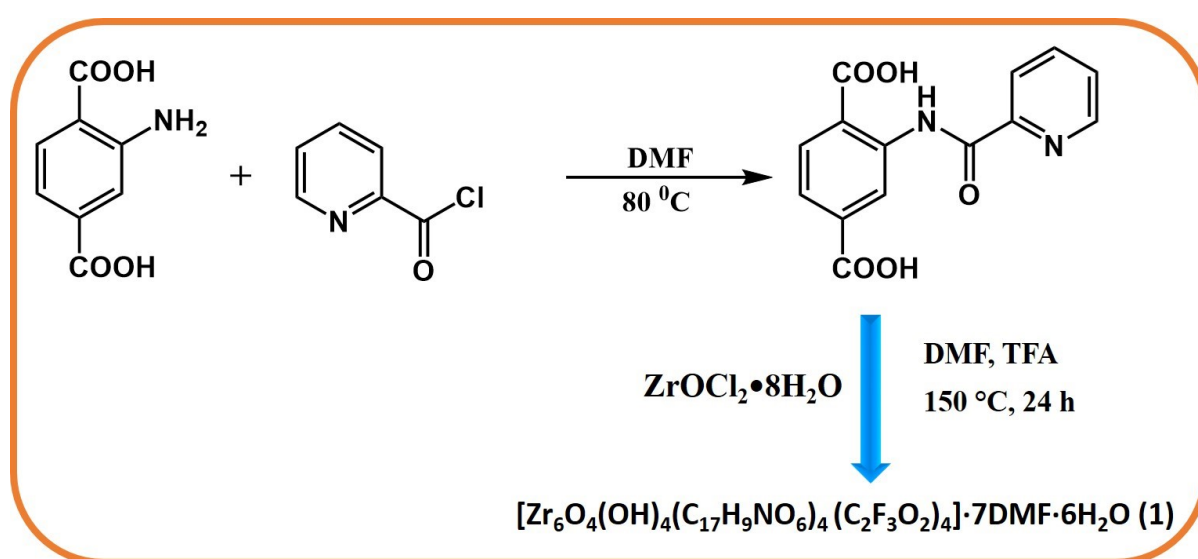
Preparation of MOF (1') Suspension for Fluorescence Sensing Experiments:

The sensing experiments were performed in aqueous medium for both the analytes. The aqueous suspension of MOF was prepared in the following way: 5 mg of probe **1'** was suspended in a glass vial containing 1 mL of water and placed in a sonication bath for 30 min.

After that the vial was kept overnight at room temperature to make the suspension stable. The fluorescence sensing experiment was executed using 100 μL of above-mentioned suspension in a quartz cuvette containing 3 mL of distilled water. The fluorescence data were recorded upon exciting the suspension at 330 nm. For competitive analysis, different analyte solutions (10 mM) were added to the above suspension and the emission response was recorded.

Synthesis of 2-(Benzofuran-2-Carboxamido)Terephthalic Acid (H_2L Linker):

In a 50 mL round-bottom flask, 2-amino-1,4-benzenedicarboxylic acid (362 mg, 2 mmol) and benzofuran-2-carbonyl chloride (360 mg, 6 mmol) were taken. Then, 10 mL of dry DMF was added to the mixture and stirred for 24h at 80 $^\circ\text{C}$ under N_2 atmosphere. After completion of the reaction, the reaction mixture was poured into ice cold water and precipitation was obtained. The product was collected by filtration and washing was carried out several times with water. Finally, the precipitate was dried in a hot air oven for 12 h at 80 $^\circ\text{C}$. Yield: 497 mg (1.53 mmol, 76%). The ^1H NMR and ^{13}C NMR spectra were recorded, which are depicted in Figures S1-S2. The mass spectrum of the synthesized ligand is given in Figure S3. ^1H NMR (500 MHz, DMSO-d_6): δ 12.48 (s, 1H), 9.29 (d, $J = 1.4$ Hz, 1H), 8.16 (d, $J = 8.2$ Hz, 1H), 7.84 (d, $J = 7.8$ Hz, 1H), 7.75 (s, 2H), 7.68 (s, 1H), 7.54 (s, 1H), 7.39 (s, 1H). ^{13}C NMR (125 MHz, DMSO-d_6 , ppm) 169.7, 166.9, 156.8, 154.9, 148.8, 140.7, 136.1, 132.1, 128.1, 127.7, 124.5, 123.6, 121.2, 112.3, 112.1. HR-MS (m/z): 326.0682 for ($\text{M}+\text{H}$)- ion.



Scheme S1. Reaction scheme for the synthesis of H_2L linker and MOF (1).

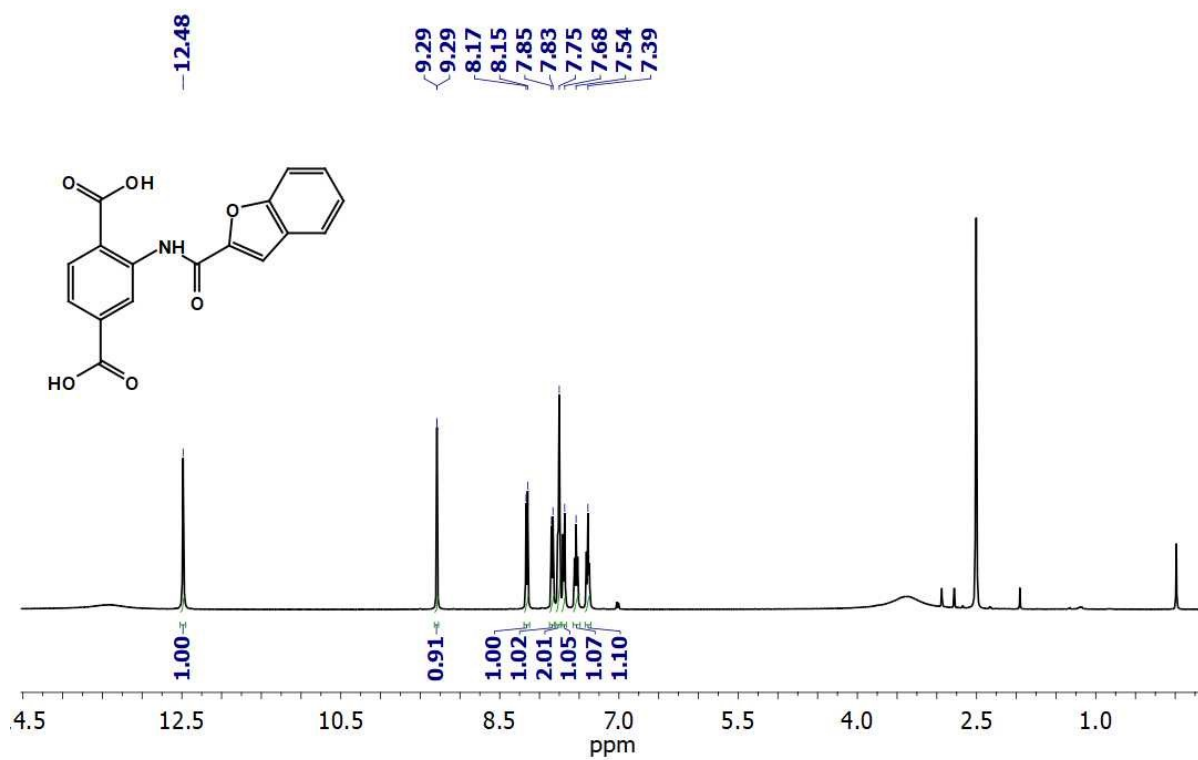


Figure S1. 1H NMR spectrum (500 MHz, DMSO- d_6) of H_2L linker.

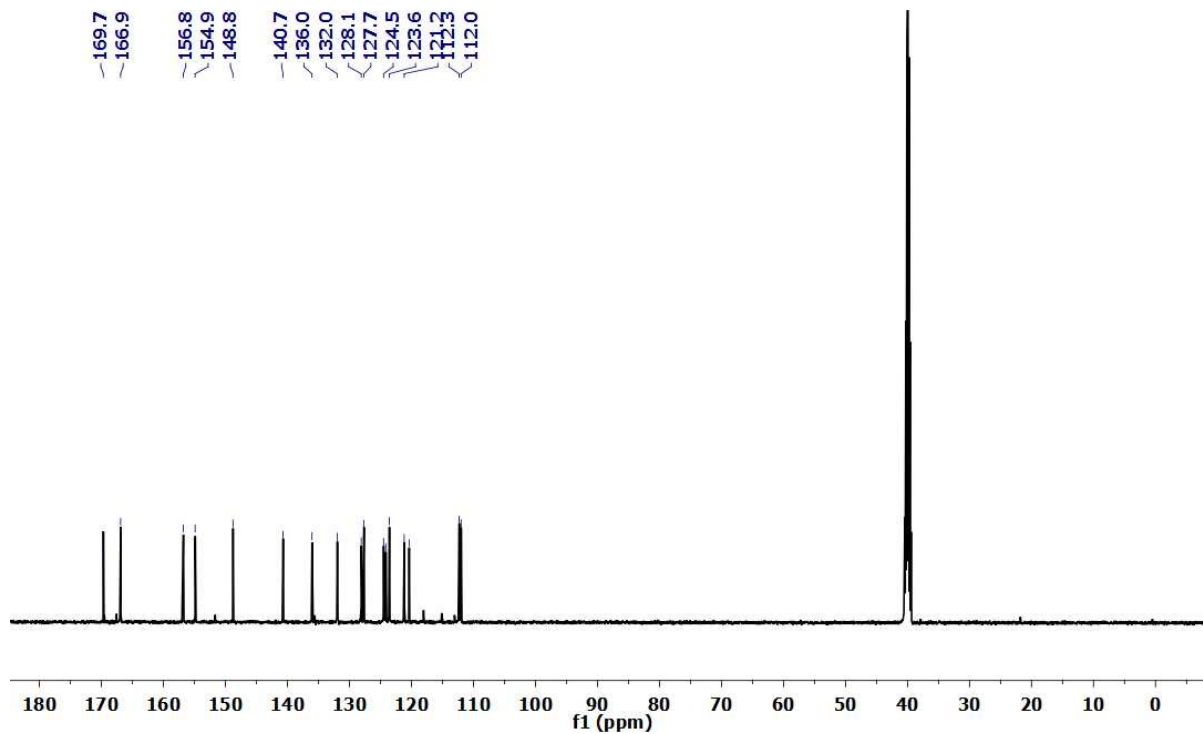


Figure S2. ^{13}C NMR spectrum (125 MHz, DMSO- d_6) of H_2L linker.

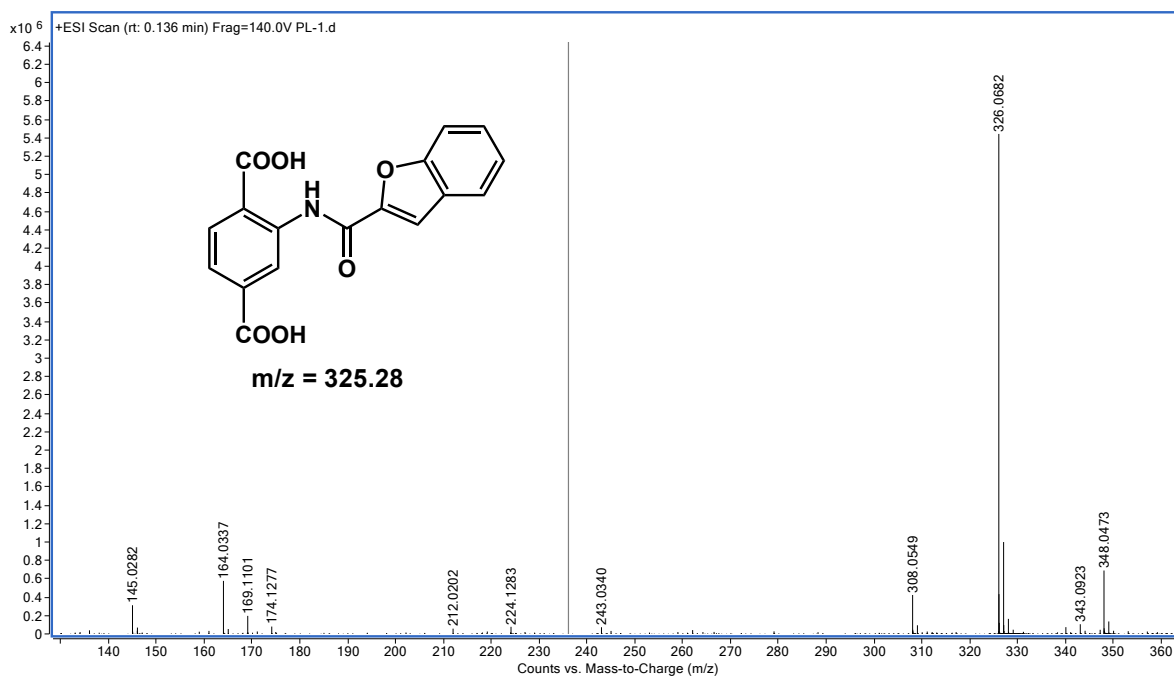


Figure S3. ESI-MS spectrum of H_2L linker measured in methanol. The spectrum shows m/z peak at 326.0682, which corresponds to $(M+H)^+$ ion [M = mass of 2-(2-methoxy-2-oxoacetamido)terephthalic acid linker].

Table S1. Unit cell parameters of $1'$ obtained by indexing its PXRD data. The obtained values have been compared with parent UiO-66 MOF.

Compound Name	$1'$	UiO-66 ¹
Crystal System	Cubic	Cubic
$a = b = c$ (Å)	20.7485(12)	20.7004(2)
V (Å ³)	8932.2(9)	8870.3(2)

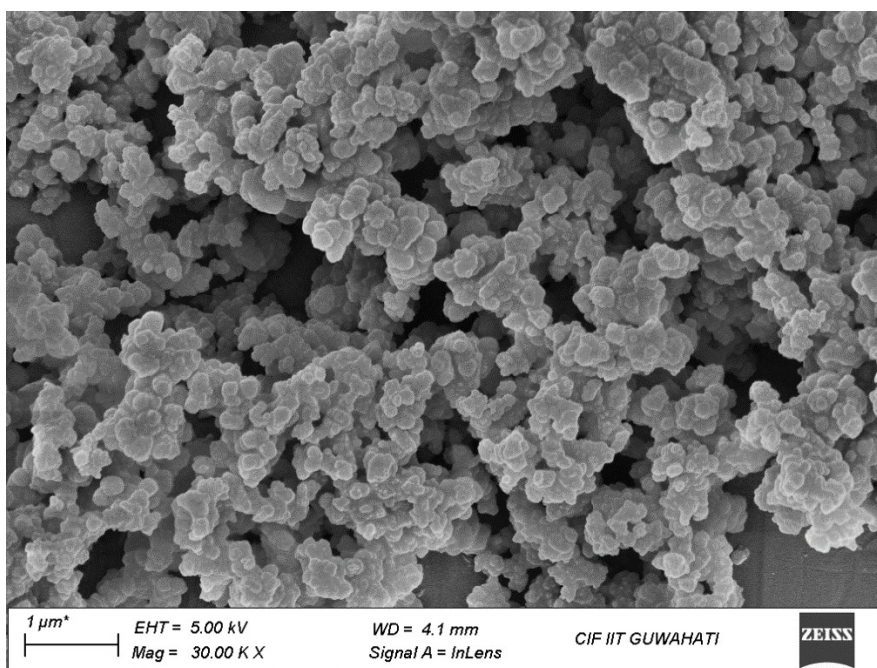


Figure S4. Field emission scanning electron microscopy image of **1'**.

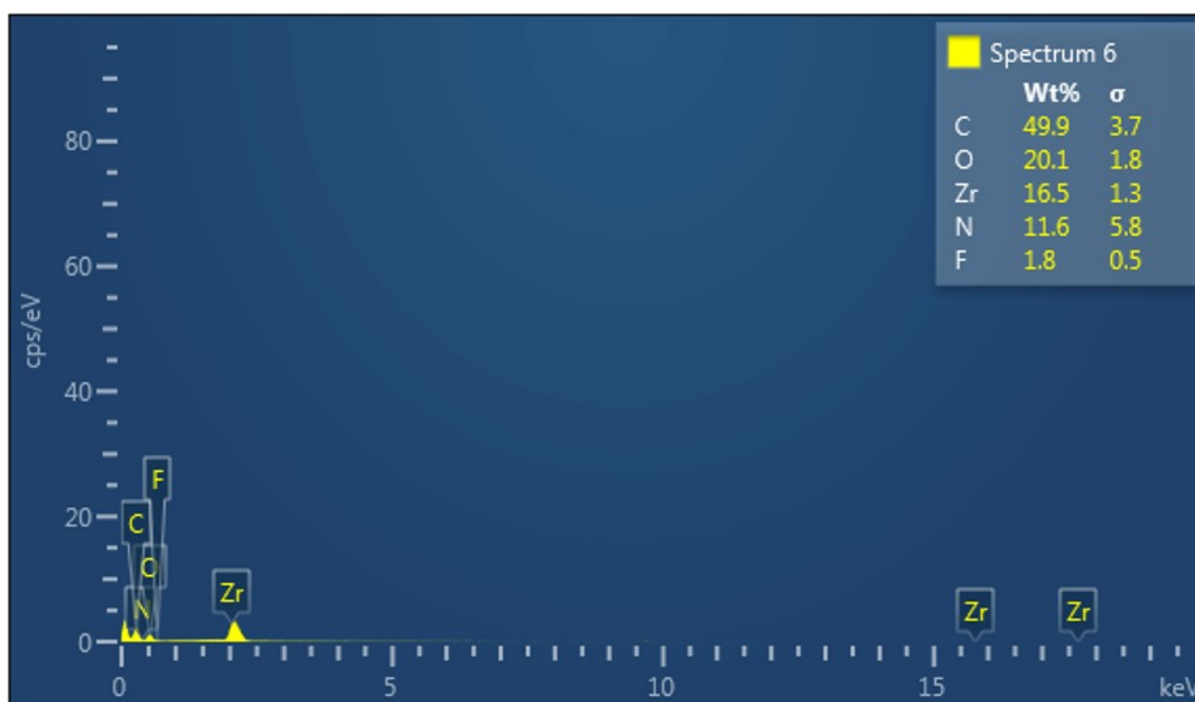


Figure S5. EDX spectrum of **1'**.

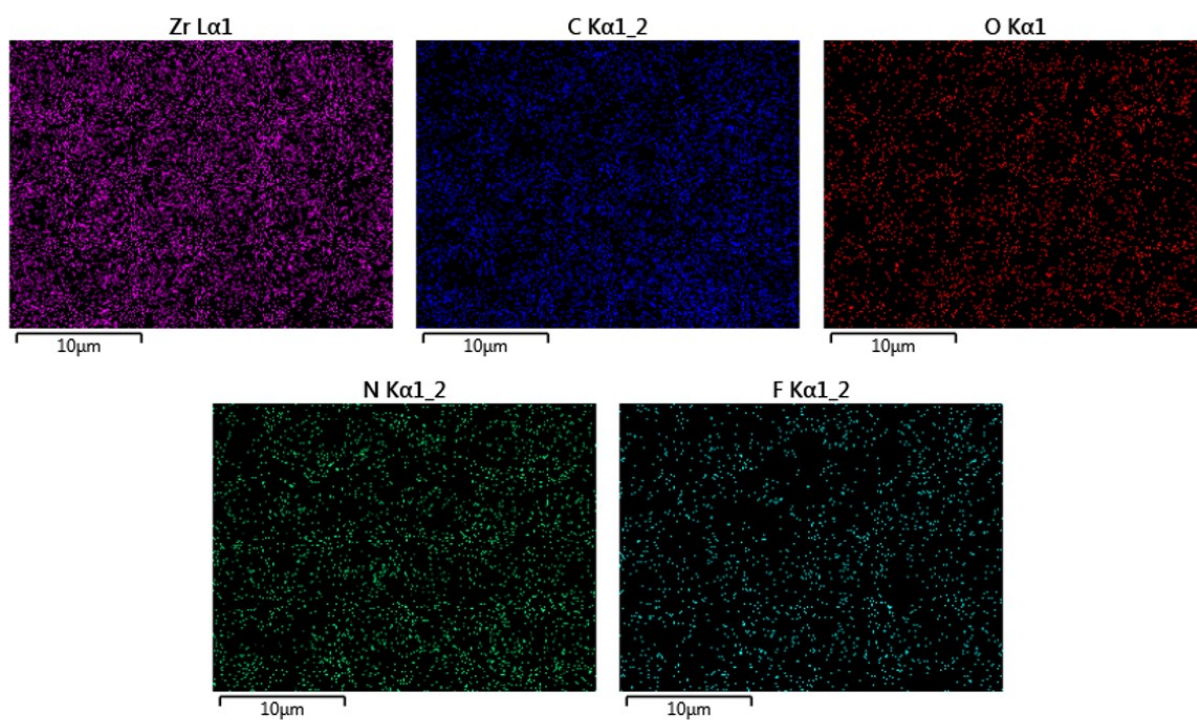


Figure S6. EDX elemental mapping of expected elements present in 1'.

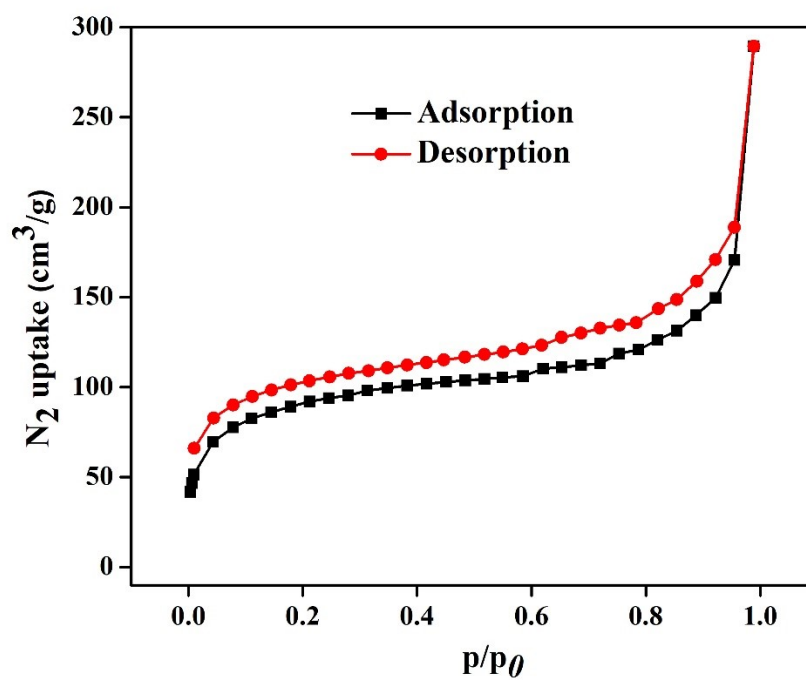


Figure S7. N₂ sorption isotherms of 1' measured at -196 °C.

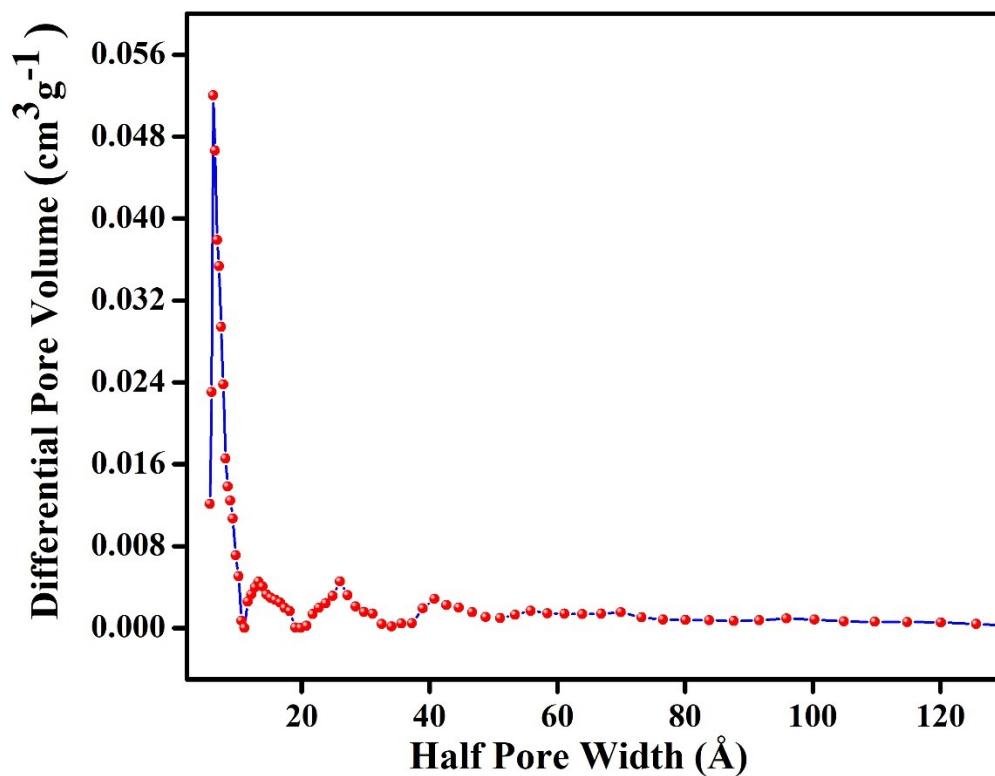


Figure S8. Density functional theory pore-size distribution of compound **1'** as determined from its N₂ adsorption isotherms at -196 °C.

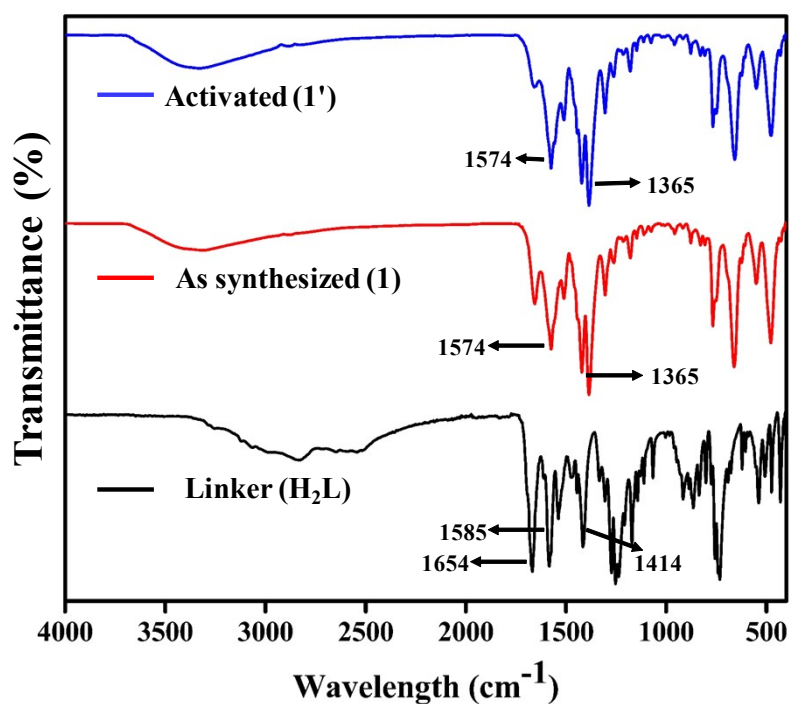


Figure S9. ATR-IR spectra of H₂L linker, **1** and **1'**.

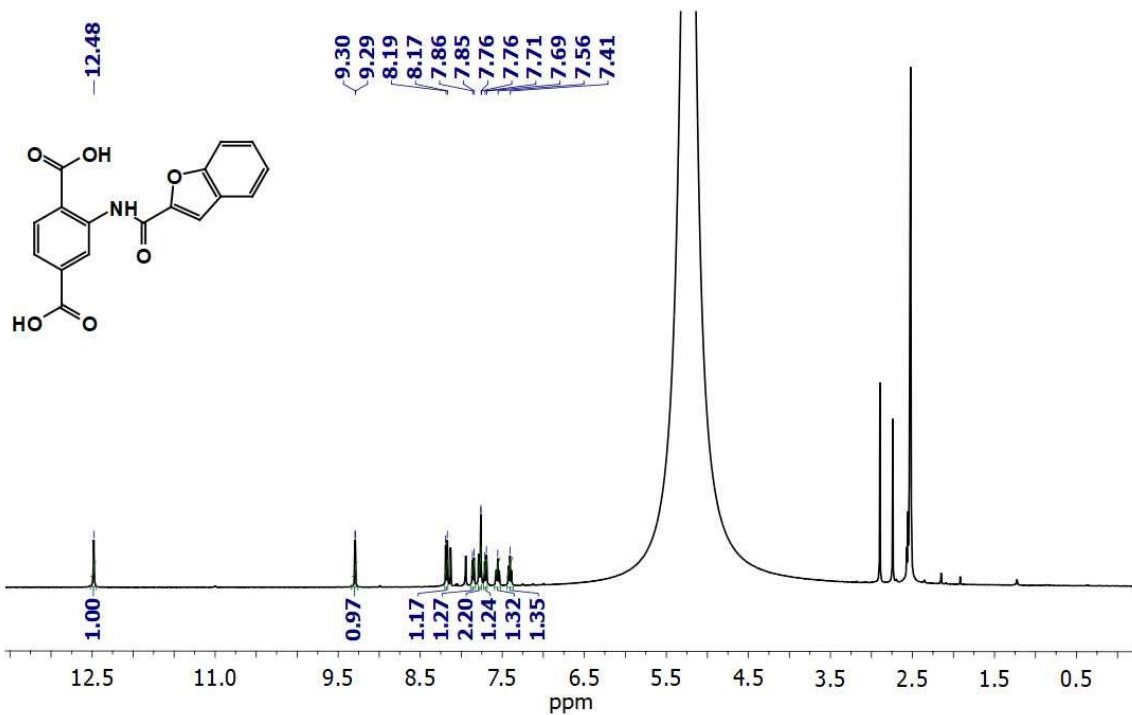


Figure S10. ^1H NMR spectrum of digested 1' (MOF was digested using 20 μL of 40% HF in 500 μL of DMSO-d_6).

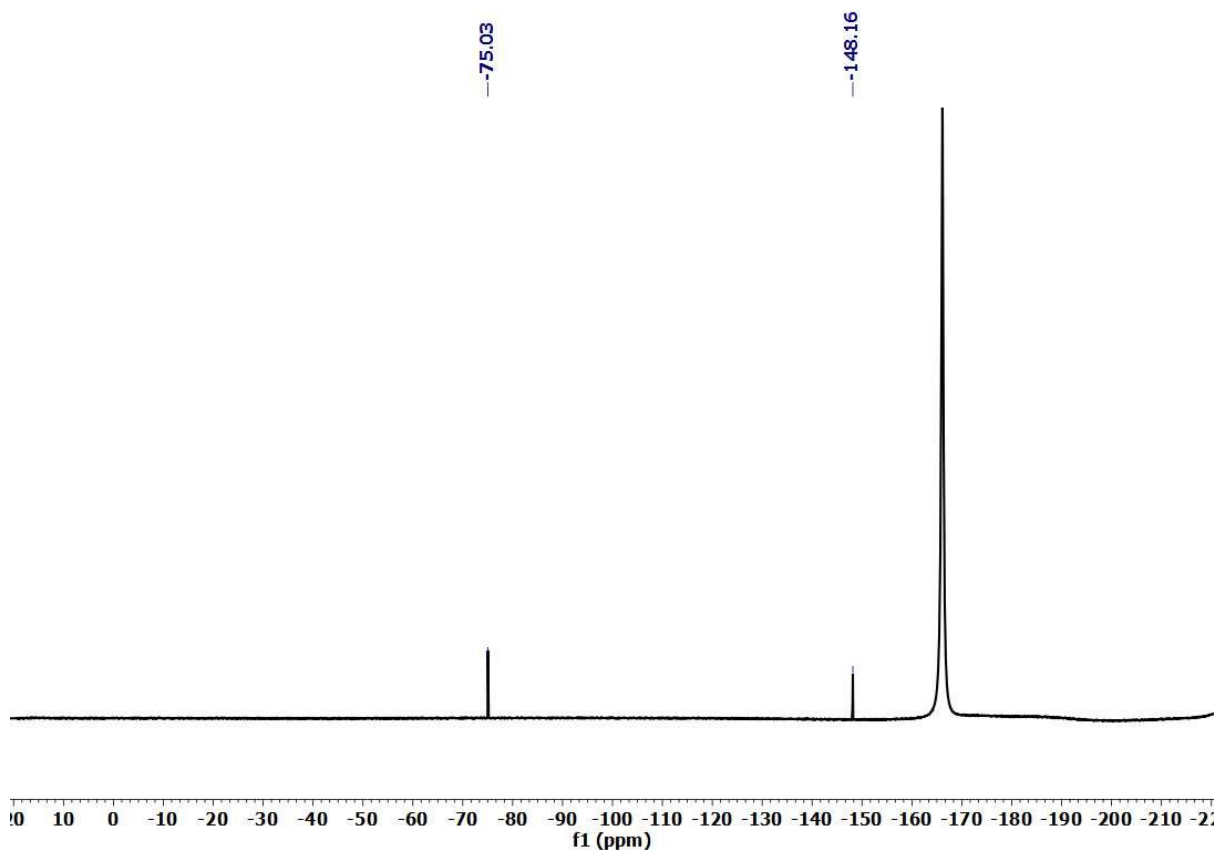


Figure S11. ^{19}F NMR spectrum of digested 1' (MOF was digested using 20 μL of 40% HF in 500 μL of DMSO-d_6).

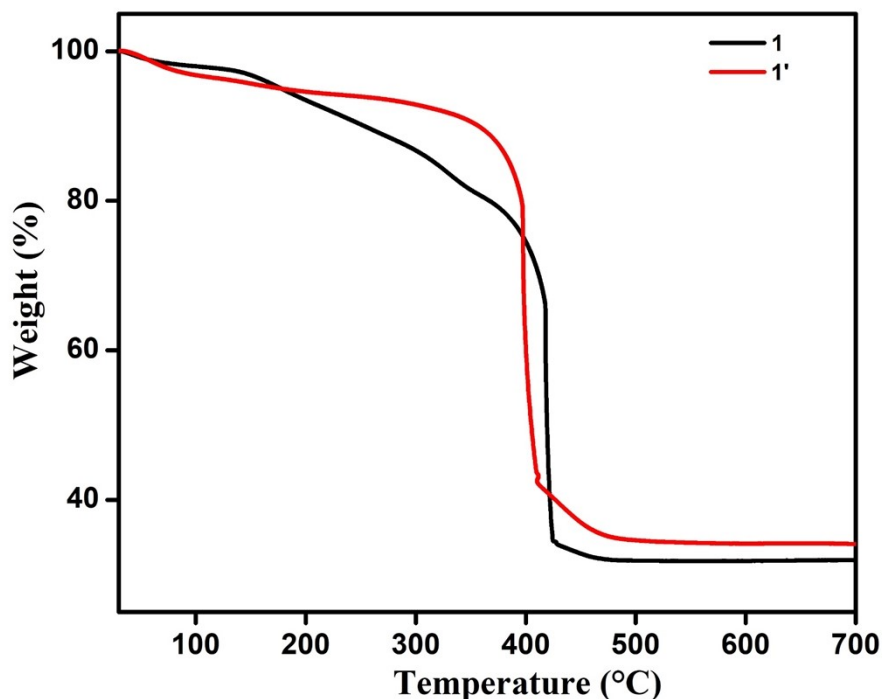


Figure S12. Thermogravimetric analysis curves of as-synthesized **1** (black) and thermally activated **1'** (red) recorded under O₂ atmosphere in the temperature range of 30-700 °C with a heating rate of 4 °C min⁻¹.

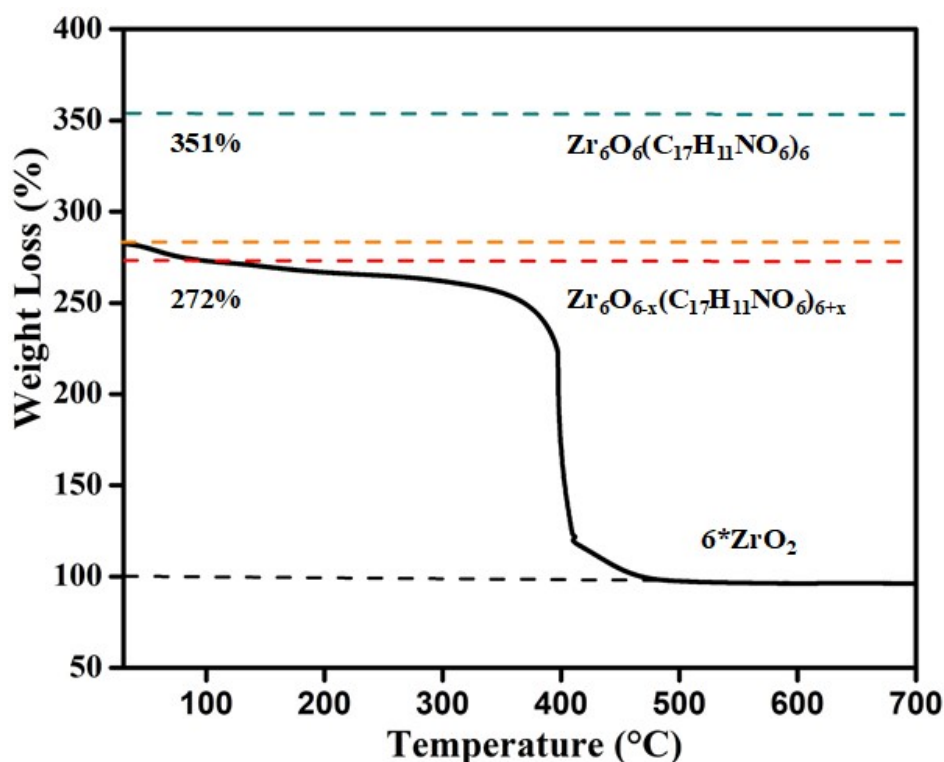
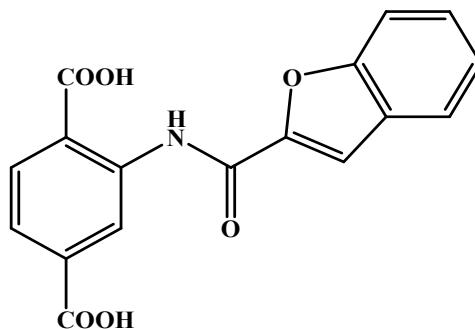


Figure S13. Calculation of missing ligand defects from the TG curve of activated **1'**. The vertical dashed line pinpoints $T_{\text{Plat.}}$, the temperature at which the plateau ($W_{\text{Exp. Plat.}}$) is reached. The horizontal dashed lines pinpoint the relevant TGA plateaus.

Calculation of Linker Defects for Zr-BDC-NH-Me MOF from TGA Data:



Linker

Formula of MOF = $Zr_6(O)_4(OH)_4(C_{17}H_{11}NO_6)_6$

Molecular Weight = 2631.3g/mol

- ❖ The dehydroxylated and modulator free formula of MOF is $[(Zr_6(O)_4(OH)_4(C_{17}H_{11}NO_6)]$ (ideal),
- ❖ Molecular Weight = 2631.3 g/mol
- ❖ The dehydroxylated and modulator free formula of MOF is $[Zr_6(O)_{6+x}(C_{17}H_{11}NO_6)_{6-x}]$ (experimental), Molecular Weight = 2594.97 g/mol (x = number of linker defect).
- ❖ From TGA data, after the final weight loss step, the remaining mass is due to 6 moles of ZrO_2 i.e. $6 \times 123.2 = 739.3$ g/mol.
- ❖ The ideal Weight of $[Zr_6(O)_6(C_{10}H_{10}N_2O_4)_6]$ is 3.51 times of 6 moles of ZrO_2 .
- ❖ The remaining flat mass obtained at the last mass on TGA curve was normalized to 100%.
- ❖ The ideal normalized mass percentage for $[Zr_6(O)_6(C_{17}H_{11}NO_6)_6]$ is 351 %.
- ❖ The experimental normalized mass percentage of $[Zr_6(O)_{6+x}(C_{17}H_{11}NO_6)_{6-x}]$ from TGA is 272%.
- ❖ $x = 6 - (W_{wt. Plat} - W_{end}/W_{t.PL.Theo})$, where
- ❖ $W_{wt. Plat}$ is the (normalized) Weight of the sample at the second TGA plateau.
- ❖ W_{end} is 100 %
- ❖ $W_{t.PL.Theo} = (W_{wt. ideal Plat.} - W_{end})/NL_{ideal}$
- ❖ $NL_{ideal} = \text{number of linkers per unit formula ideally (6)}$
- ❖ $W_{t.PL.Theo} = ((351-100)/6) = 41.8\%$
- ❖ $x = 6 - ((272 - 100)/41.8) = 6 - 4.13 = 1.86$
- ❖ The number of linker defects per unit formula is 1.86.

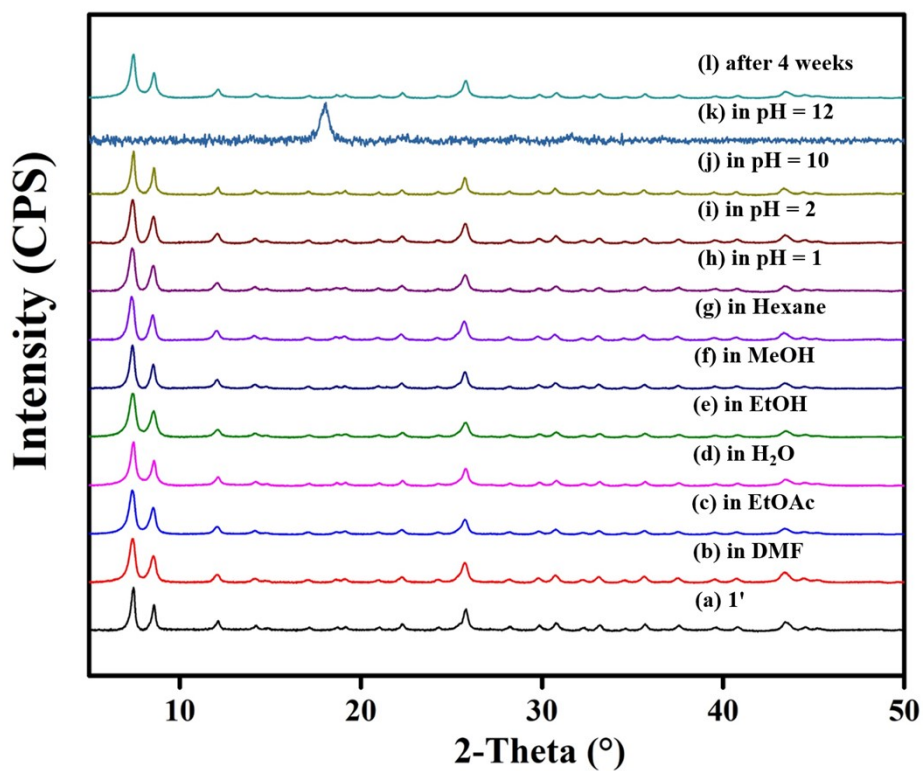


Figure S14. PXRD patterns of **1'** and the obtained samples of **1'** after stirring in different conditions for 24 h.

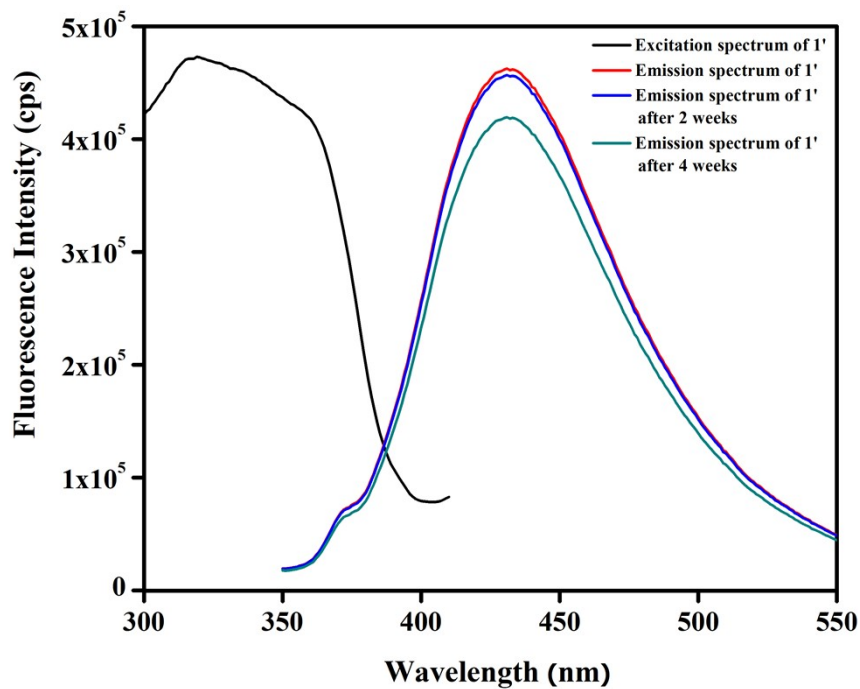


Figure S15. Fluorescence excitation and emission spectra of **1'** in HEPES buffer (pH = 7.4).

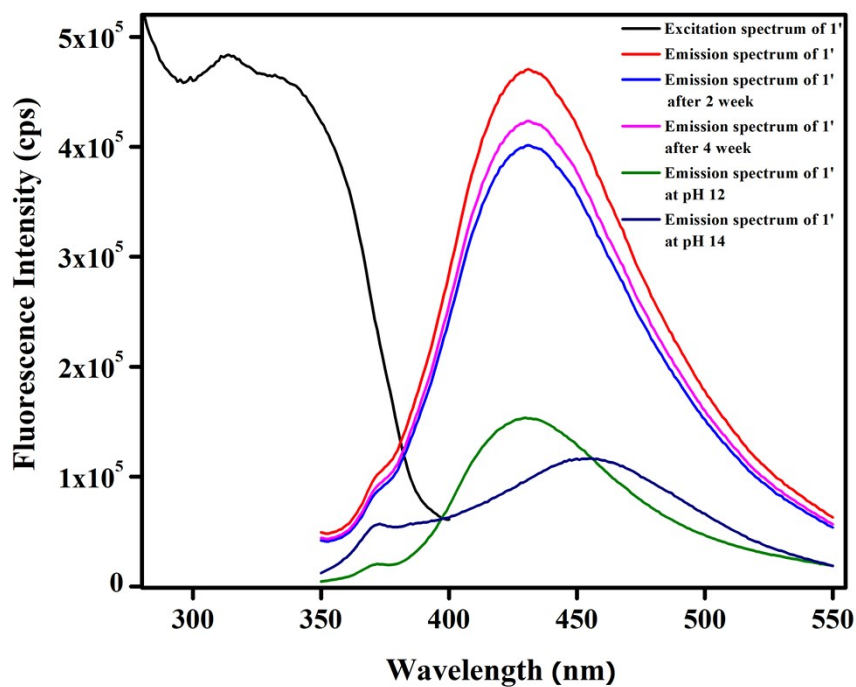


Figure S16. Fluorescence excitation and emission spectra of **1'** in water.

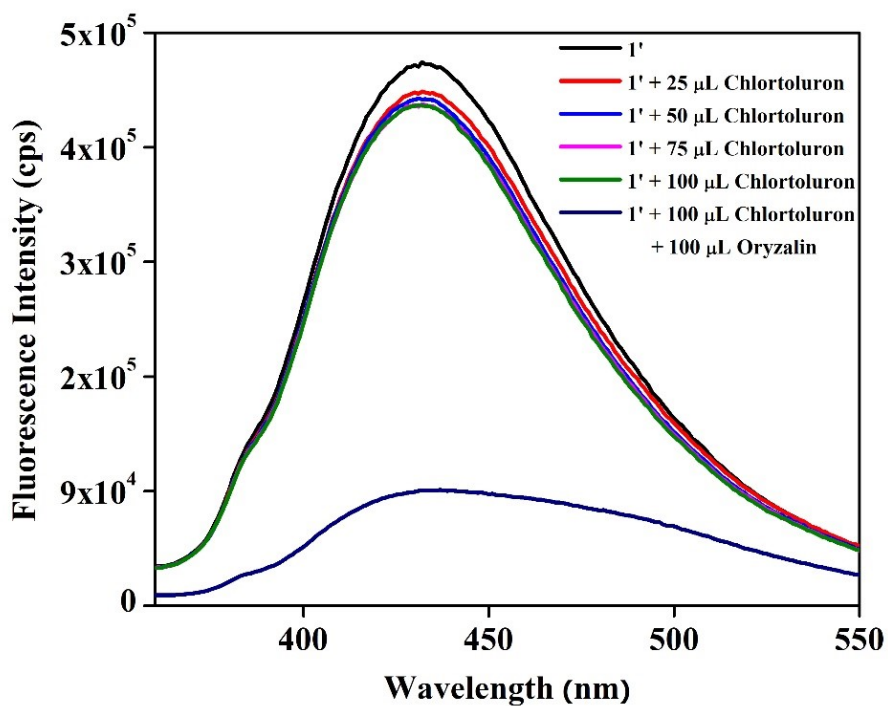


Figure S17. Quenching in fluorescence emission intensity of the suspension of **1'** in aqueous medium after addition of 100 μL of 10 mM (625 μM) aqueous oryzalin solution in presence of 100 μL of 10 mM (322 μM) aqueous solution of chlortoluron.

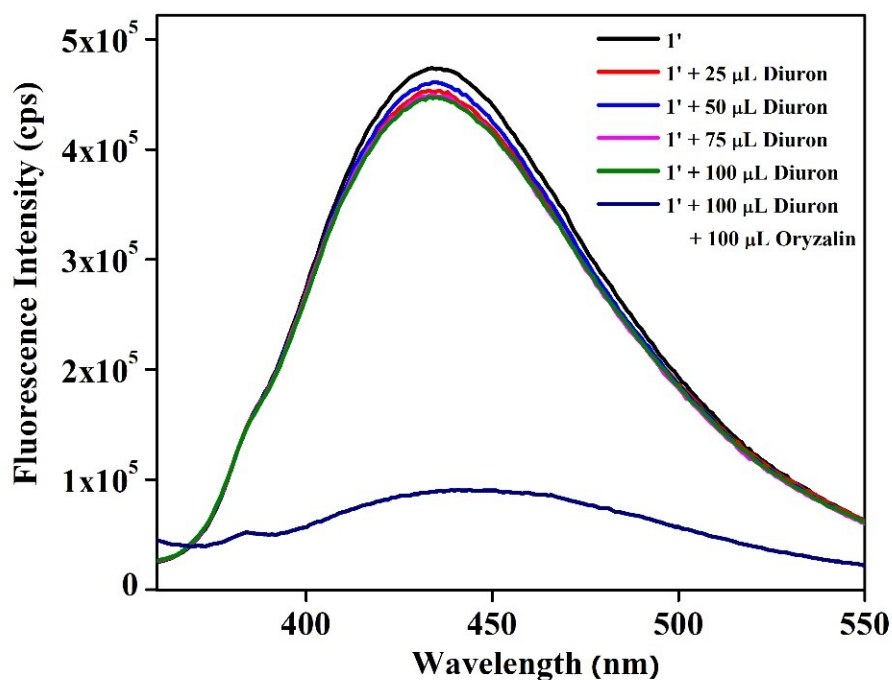


Figure S18. Quenching in fluorescence emission intensity of the suspension of **1'** in aqueous medium after addition of 100 μL of 10 mM (625 μM) oryzalin solution in presence of 100 μL of 10 mM (322 μM) aqueous solution of diuron.

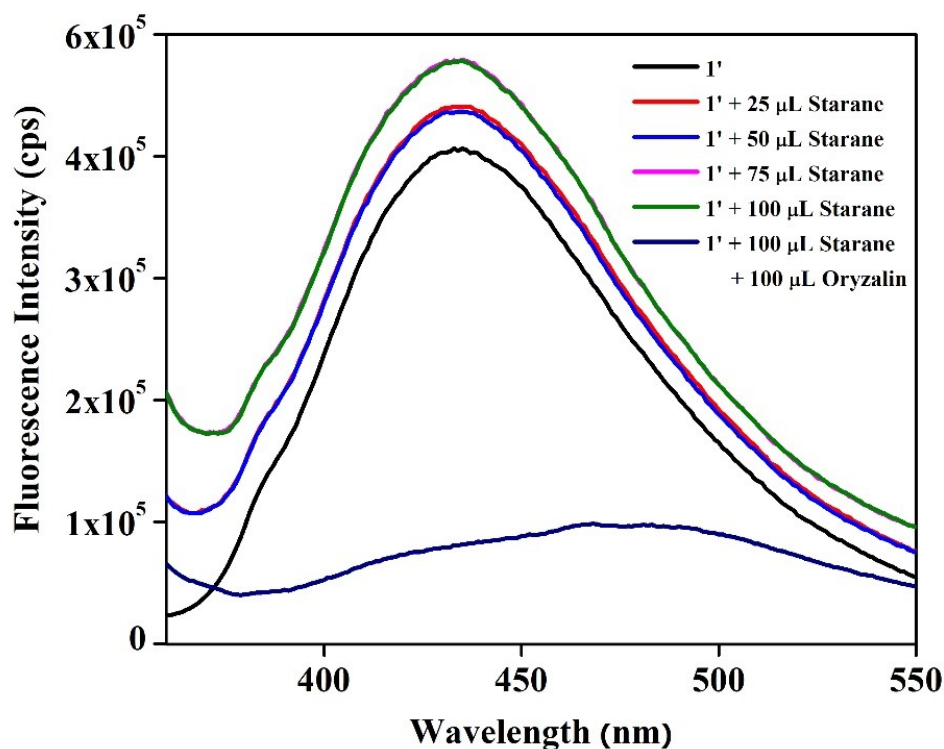


Figure S19. Quenching in fluorescence emission intensity of the suspension of **1'** in aqueous medium after addition of 100 μL of 10 mM (625 μM) oryzalin solution in presence of 100 μL of 10 mM (322 μM) aqueous solution of starane.

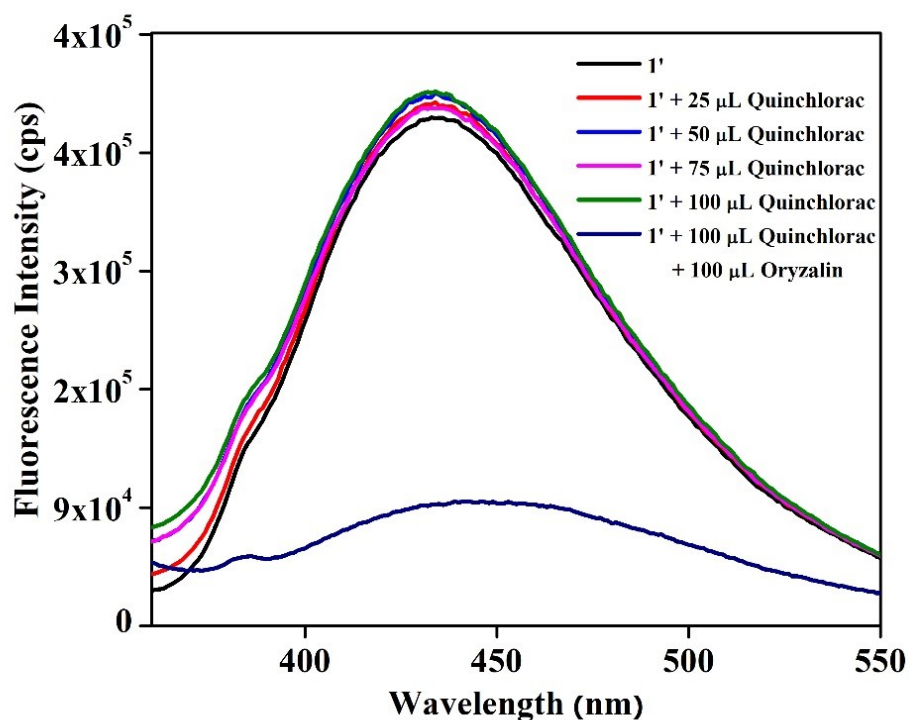


Figure S20. Quenching in fluorescence emission intensity of the suspension of **1'** in aqueous medium after addition of 100 μL of 10 mM (625 μM) aqueous oryzalin solution in presence of 100 μL of 10 mM (322 μM) aqueous solution of quinchlorac.

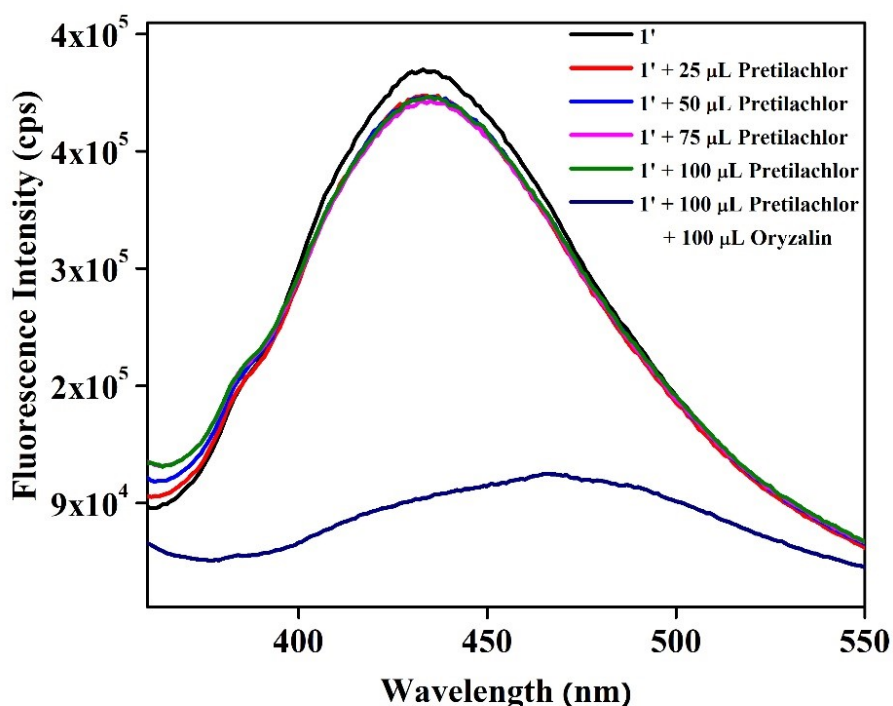


Figure S21. Quenching in fluorescence emission intensity of the suspension of **1'** in aqueous medium after addition of 100 μL of 10 mM (625 μM) aqueous oryzalin solution in presence of 100 μL of 10 mM (322 μM) aqueous solution of pretilachlor.

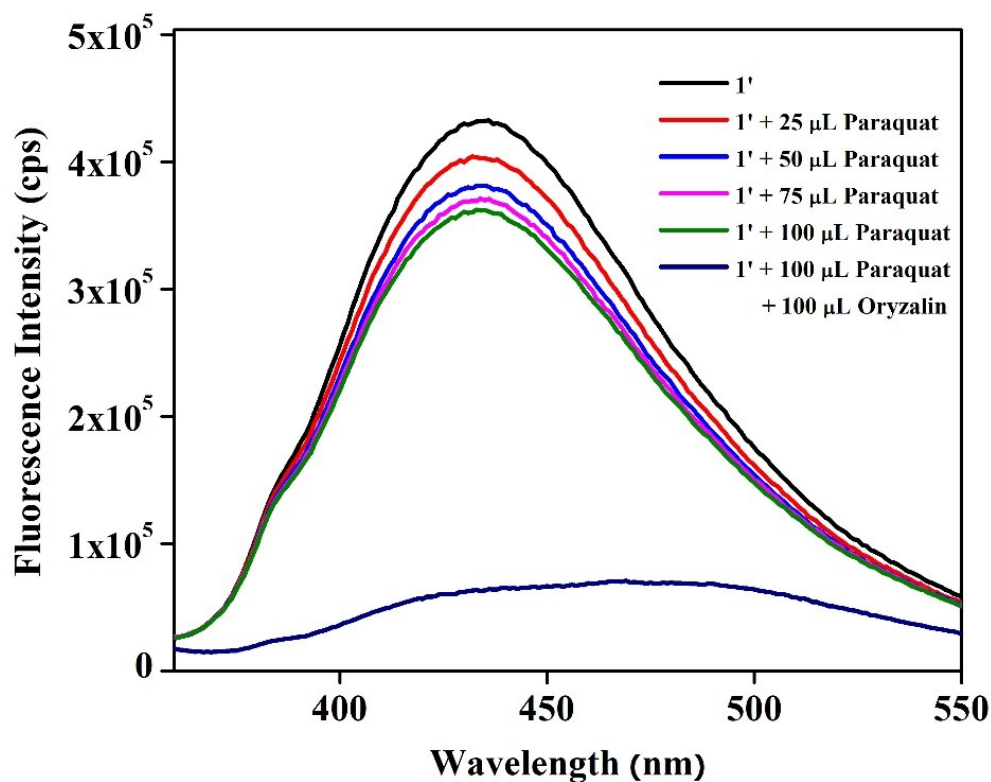


Figure S22. Quenching in fluorescence emission intensity of the suspension of **1'** in aqueous medium after addition of 100 μL of 10 mM (625 μM) aqueous oryzalin solution in presence of 100 μL of 10 mM (322 μM) aqueous solution of paraquat.

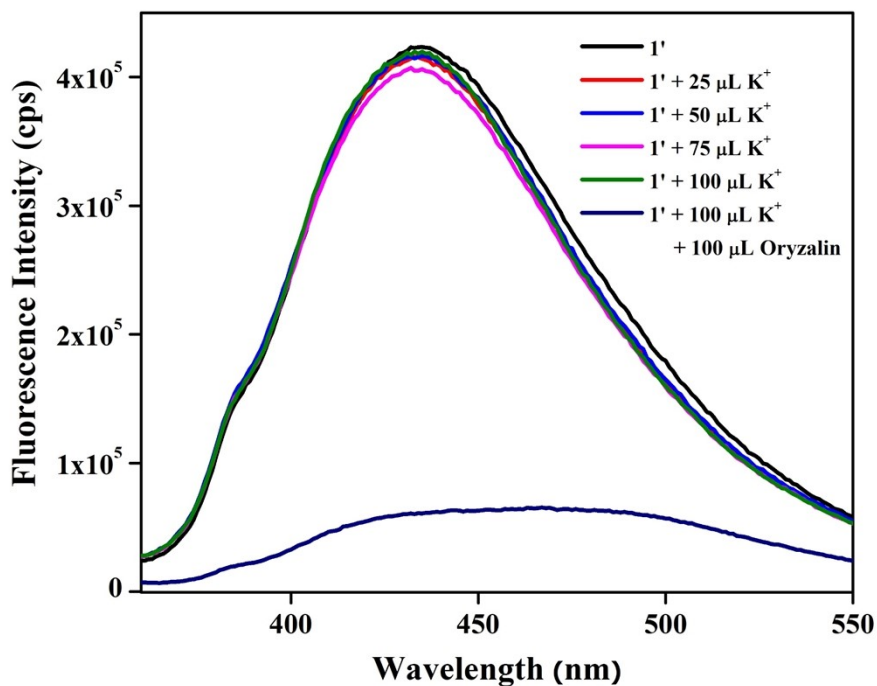


Figure S23. Quenching in fluorescence emission intensity of the suspension of **1'** in aqueous medium after addition of 100 μL of 10 mM (625 μM) aqueous oryzalin solution in presence of 100 μL of 10 mM (322 μM) aqueous solution of K^+ .

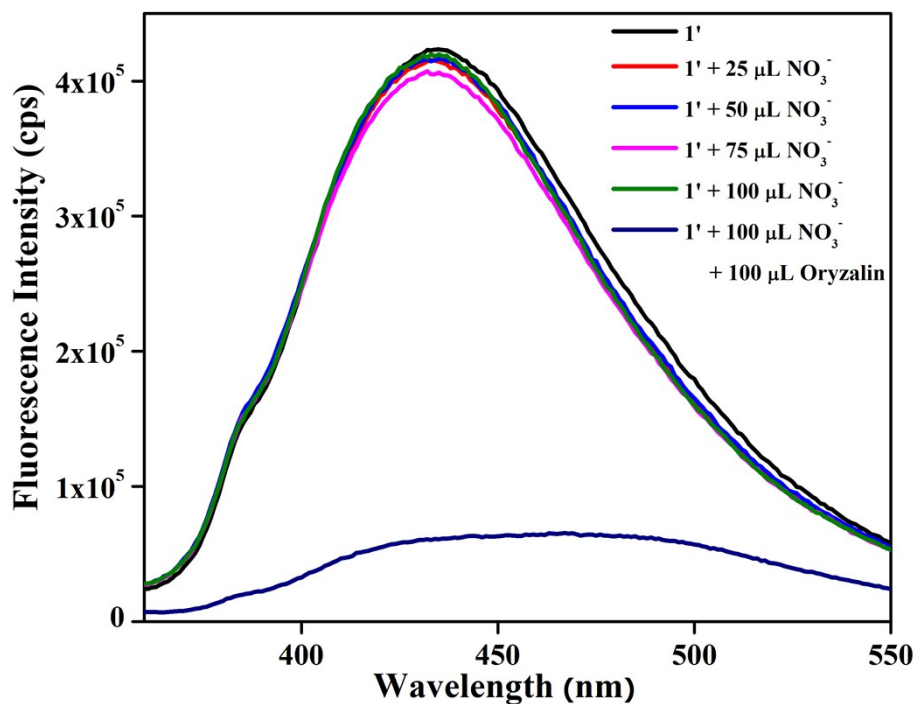


Figure S24. Quenching in fluorescence emission intensity of the suspension of **1'** in aqueous medium after addition of 100 μL of 10 mM (625 μM) aqueous ORZ solution in presence of 100 μL of 10 mM (322 μM) aqueous solution of NO_3^- .

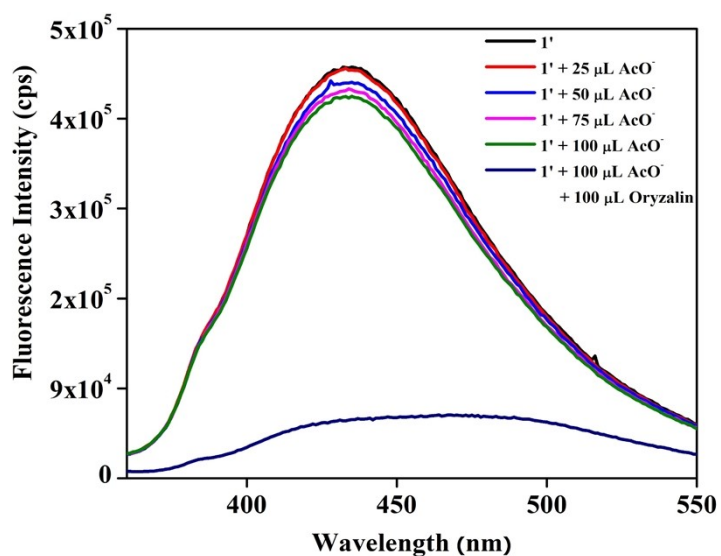


Figure S25. Quenching in fluorescence emission intensity of the suspension of **1'** in aqueous medium after addition of 100 μL of 10 mM (625 μM) aqueous oryzalin solution in presence of 100 μL of 10 mM (322 μM) aqueous solution of AcO^- .

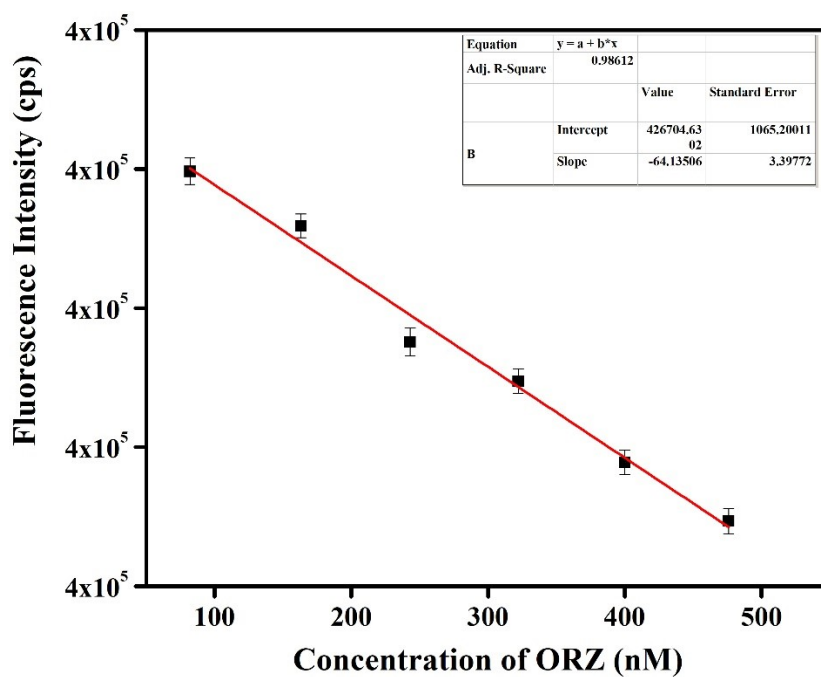


Figure S26. Change in the fluorescence emission intensity of **1'** as a function of concentration of ORZ.

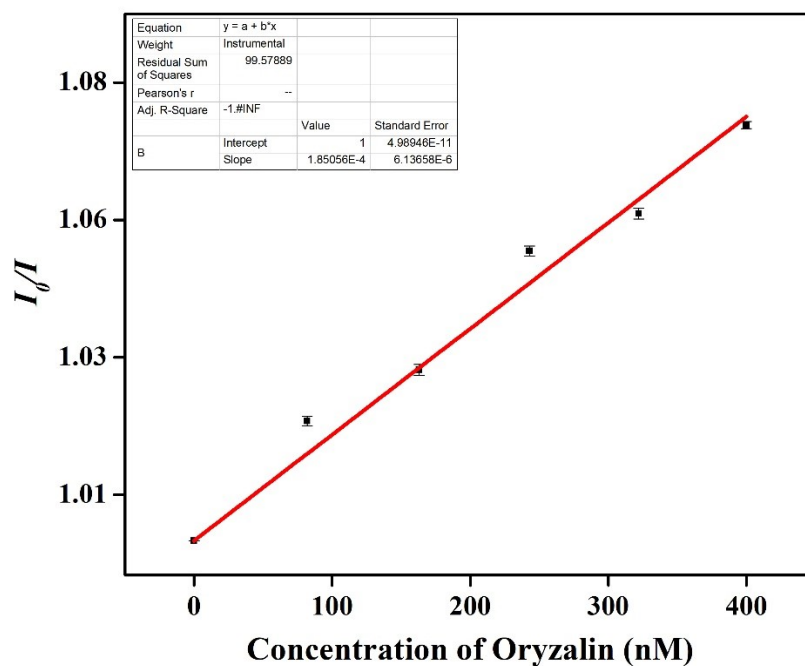


Figure S27. Stern-Volmer plot for the fluorescence emission quenching of **1'** in presence of oryzalin.

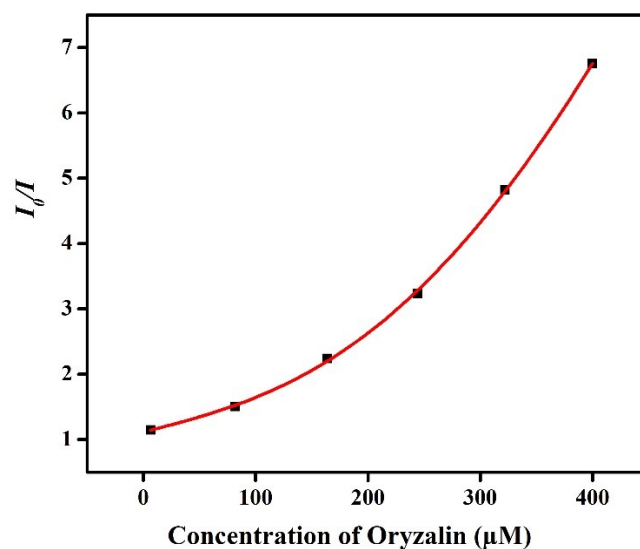


Figure S28. Stern-Volmer plot for fluorescence quenching of **1'** in aqueous medium against increasing different concentrations of ORZ.

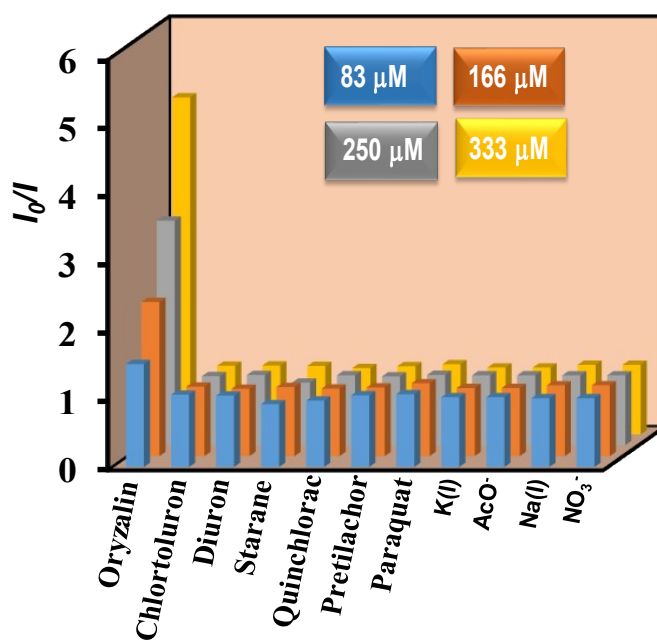


Figure S29. 3D Stern-Volmer plots for various analytes for ORZ sensing.

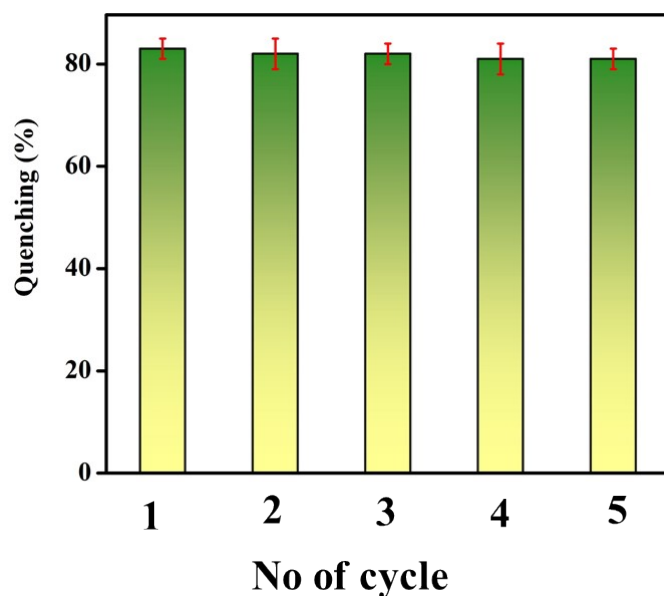


Figure S30. Recyclability test of probe **1'** for the sensing of 10 mM (322 μ M) oryzalin in aqueous medium.

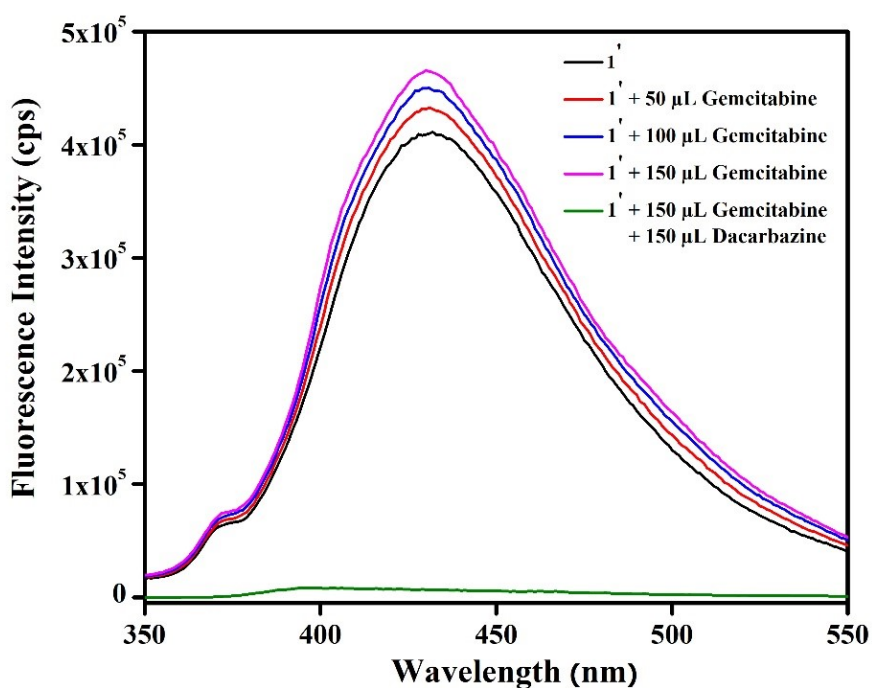


Figure S31. Quenching in fluorescence emission intensity of the suspension of **1'** in HEPES buffer medium after addition of 150 μ L of 10 mM (909 μ M) dacarbazine solution in presence of 150 μ L of 10 mM (476 μ M) solution of gemcitabine.

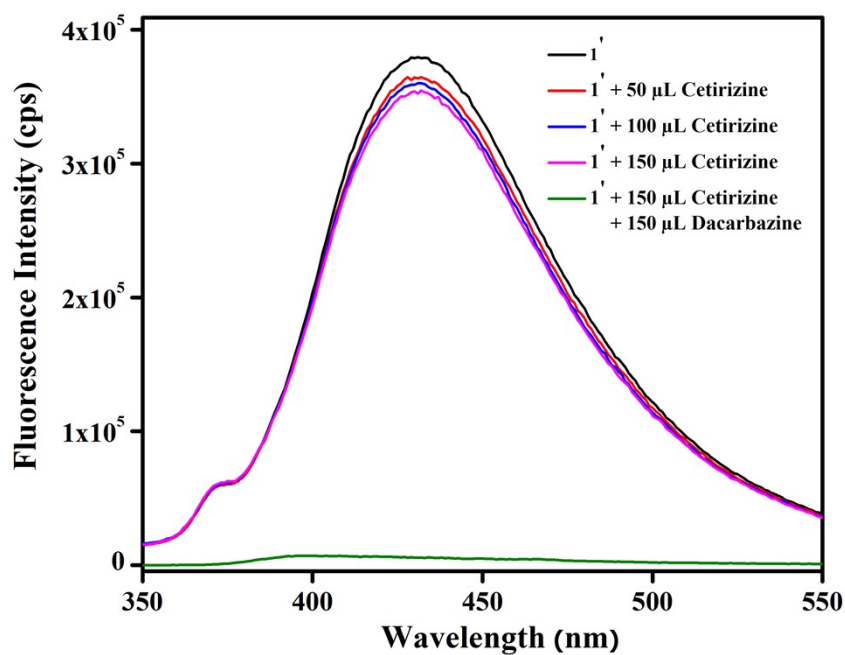


Figure S32. Quenching in fluorescence emission intensity of the suspension of 1' in HEPES buffer medium after addition of 150 μL of 10 mM (909 μM) dacarbazine solution in presence of 150 μL of 10 mM (476 μM) solution of cetirizine.

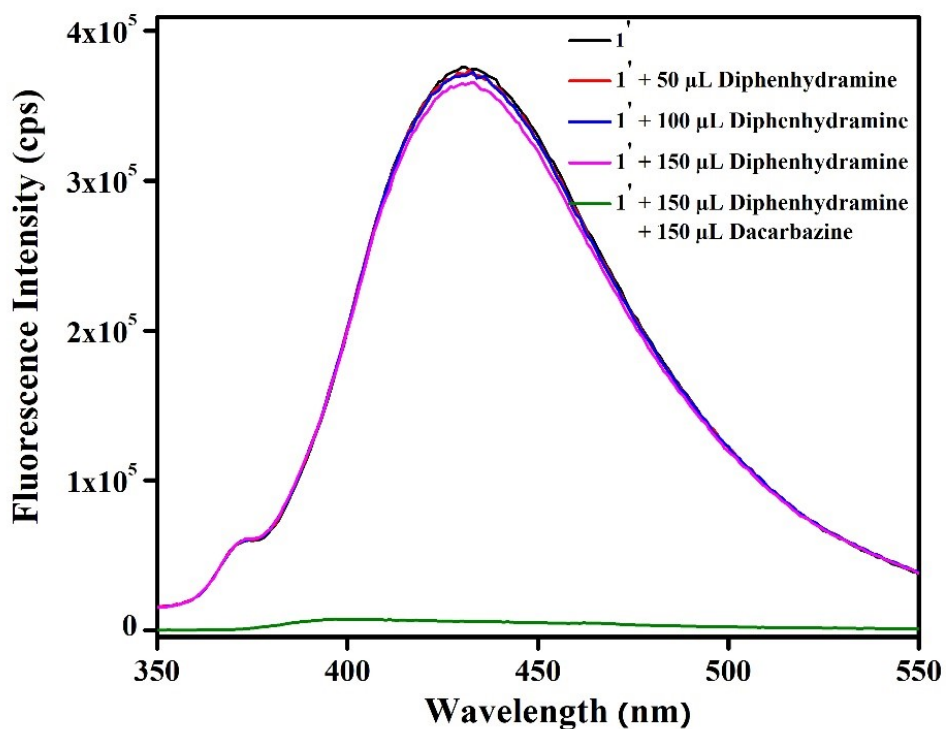


Figure S33. Quenching in fluorescence emission intensity of the suspension of 1' in HEPES buffer medium after addition of 150 μL of 10 mM (909 μM) dacarbazine solution in presence of 150 μL of 10 mM (476 μM) solution of diphenhydramine.

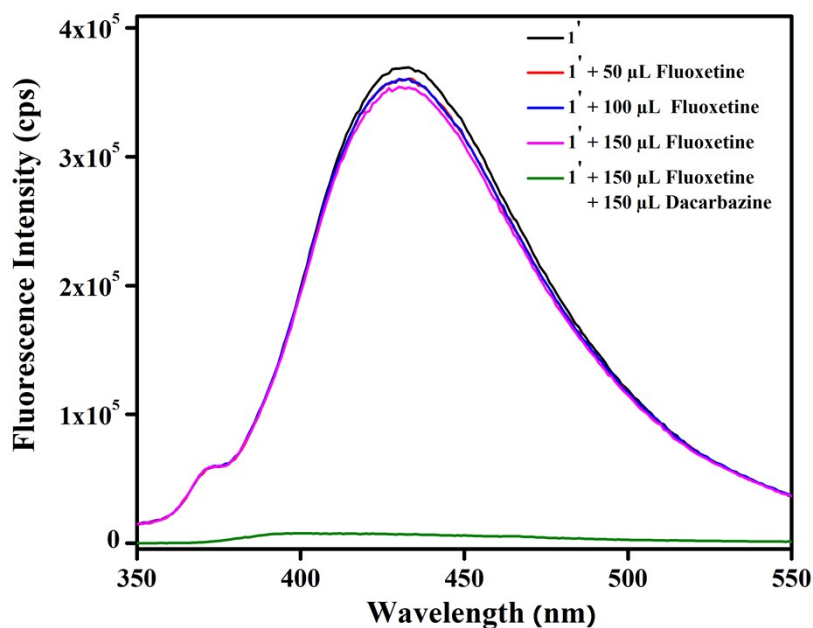


Figure S34. Quenching in fluorescence emission intensity of the suspension of **1'** in HEPES buffer medium after addition of 150 μ L of 10 mM (909 μ M) dacarbazine solution in presence of 150 μ L of 10 mM (476 μ M) solution of fluoxetine.

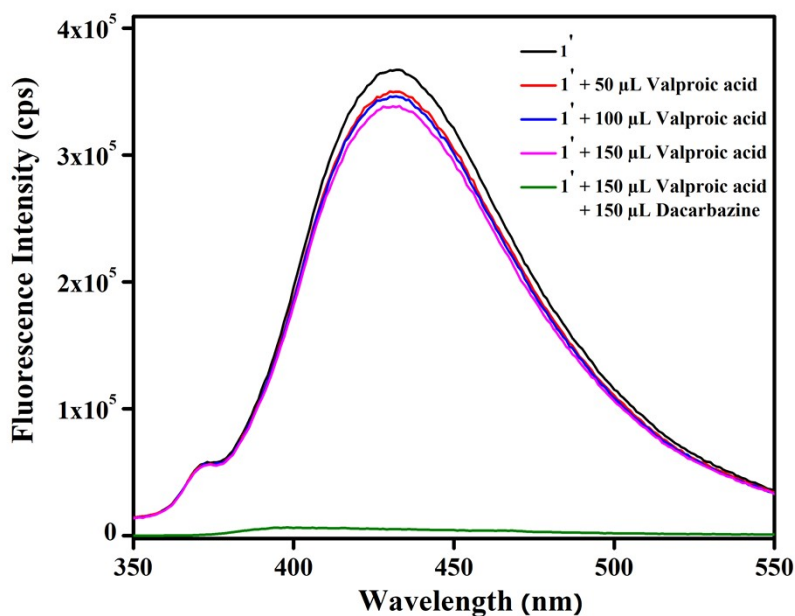


Figure S35. Quenching in fluorescence emission intensity of the suspension of **1'** in HEPES buffer medium after addition of 150 μ L of 10 mM (909 μ M) dacarbazine solution in presence of 150 μ L of 10 mM (476 μ M) solution of valproic acid.

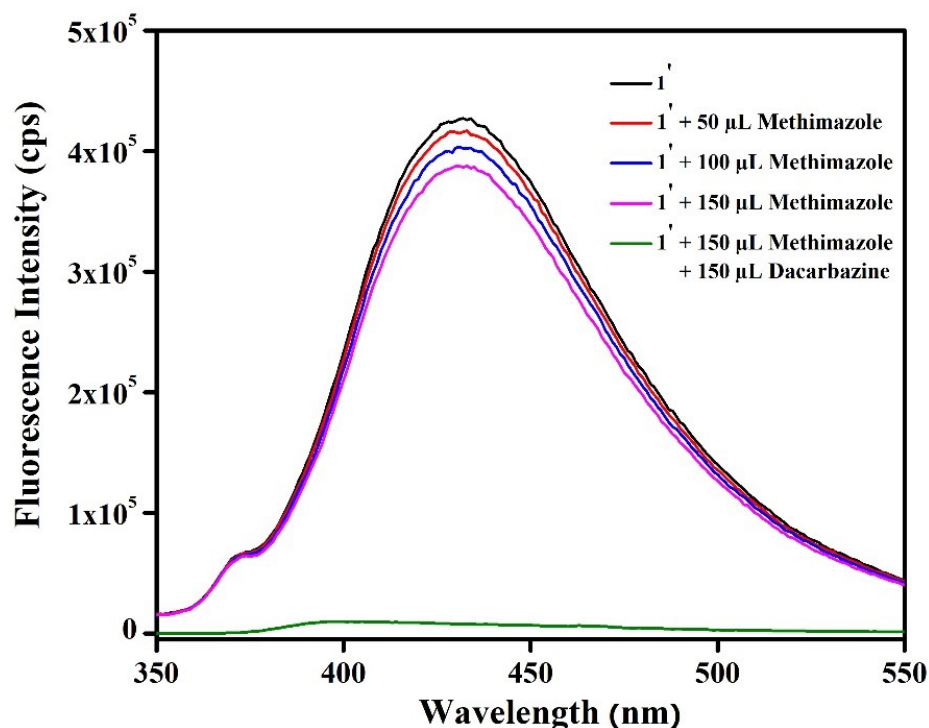


Figure S36. Quenching in fluorescence emission intensity of the suspension of 1' in HEPES buffer medium after addition of 150 μ L of 10 mM (909 μ M) dacarbazine solution in presence of 150 μ L of 10 mM (476 μ M) solution of methimazole.

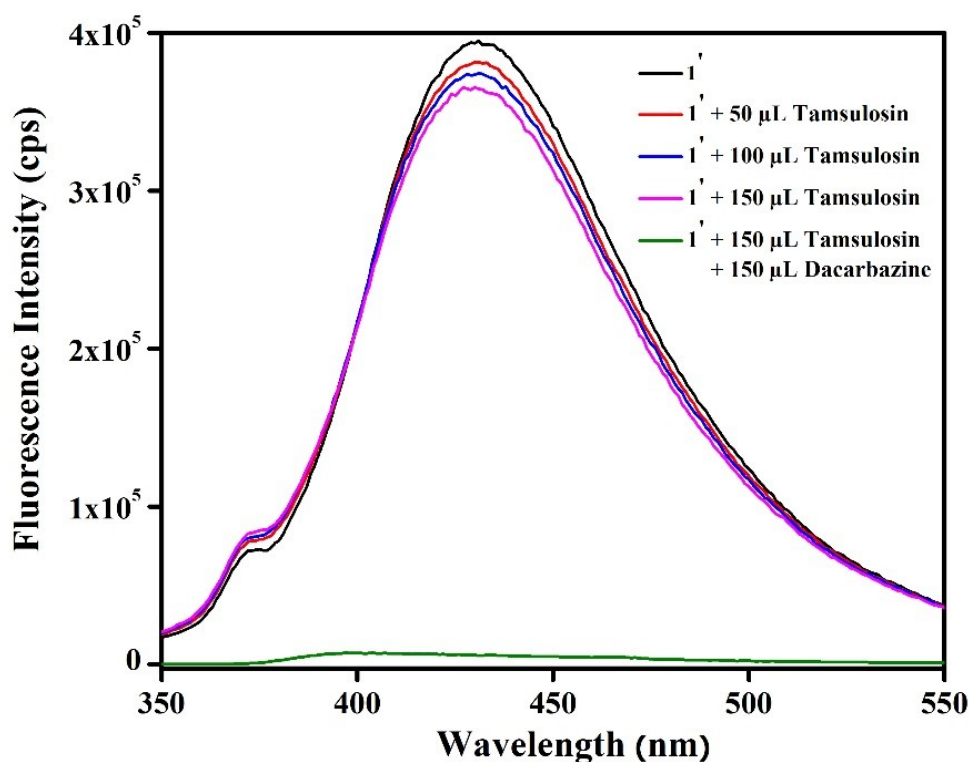


Figure S37. Quenching in fluorescence emission intensity of the suspension of 1' in HEPES buffer medium after addition of 150 μ L of 10 mM dacarbazine (909 μ M) solution in presence of 150 μ L of 10 mM (476 μ M) solution of tamsulosin.

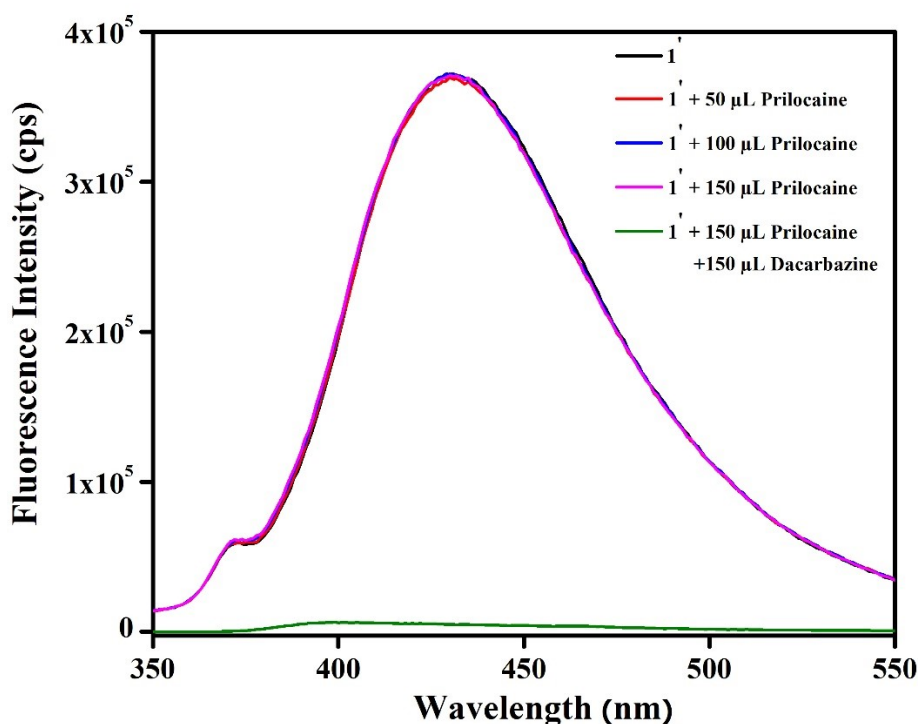


Figure S38. Quenching in fluorescence emission intensity of the suspension of **1'** in HEPES buffer medium after addition of 150 μ L of 10 mM (909 μ M) dacarbazine solution in presence of 150 μ L of 10 mM (476 μ M) solution of prilocaine.

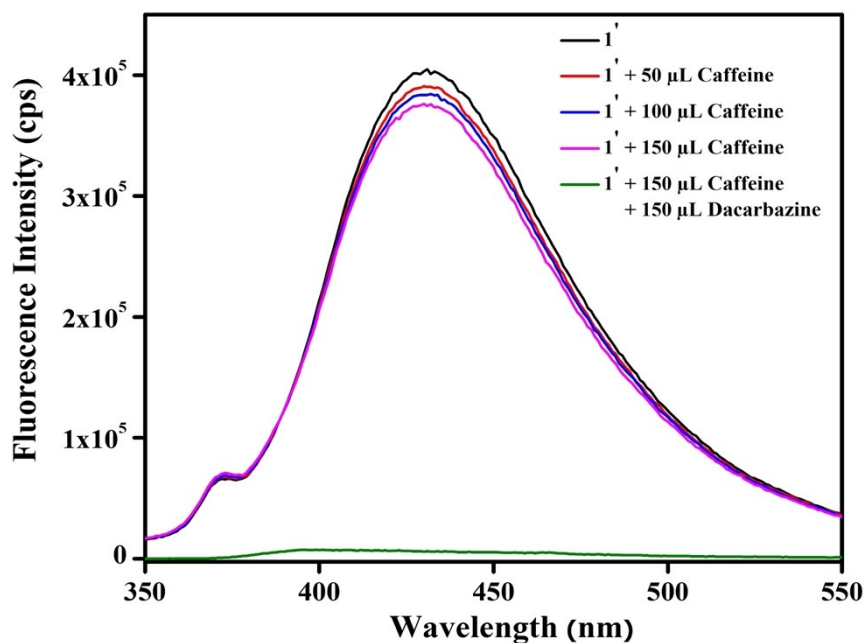


Figure S39. Quenching in fluorescence emission intensity of the suspension of **1'** in HEPES buffer medium after addition of 150 μ L of 10 mM (909 μ M) dacarbazine solution in presence of 150 μ L of 10 mM (476 μ M) solution of caffeine.

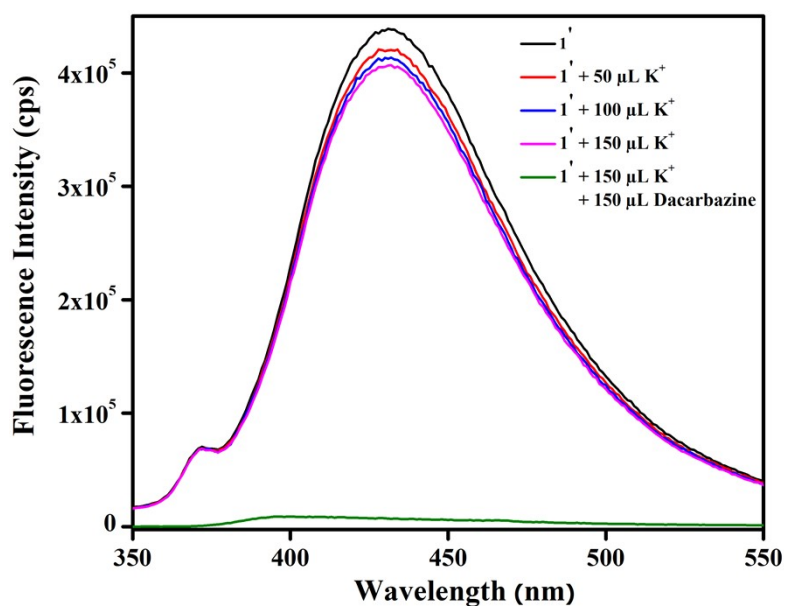


Figure S40. Quenching in fluorescence emission intensity of the suspension of **1'** in HEPES buffer medium after addition of 150 μL of 10 mM (909 μM) dacarbazine solution in presence of 150 μL of 10 mM (476 μM) solution of K⁺.

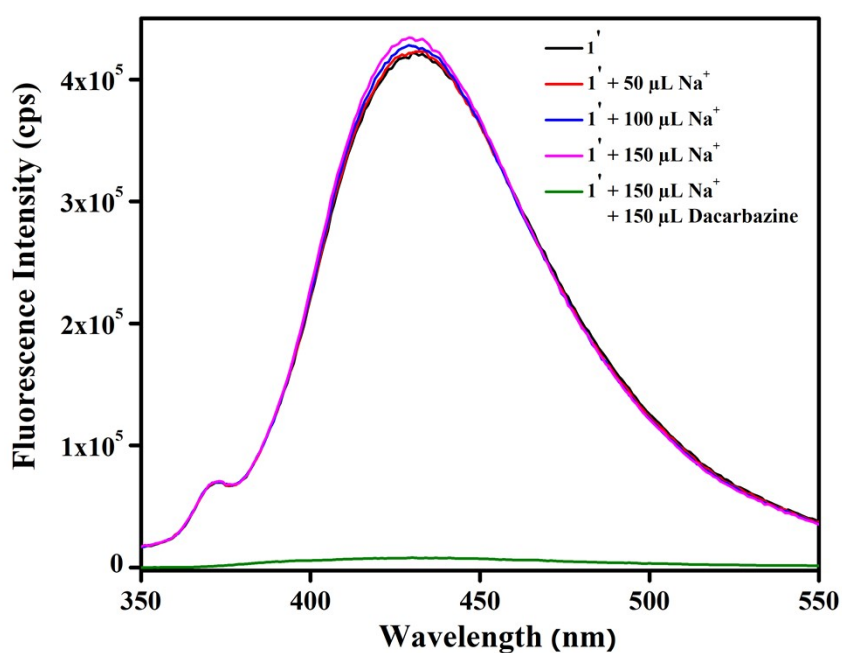


Figure S41. Quenching in fluorescence emission intensity of the suspension of **1'** in HEPES buffer medium after addition of 150 μL of 10 mM (909 μM) dacarbazine solution in presence of 150 μL of 10 mM (476 μM) solution of Na⁺.

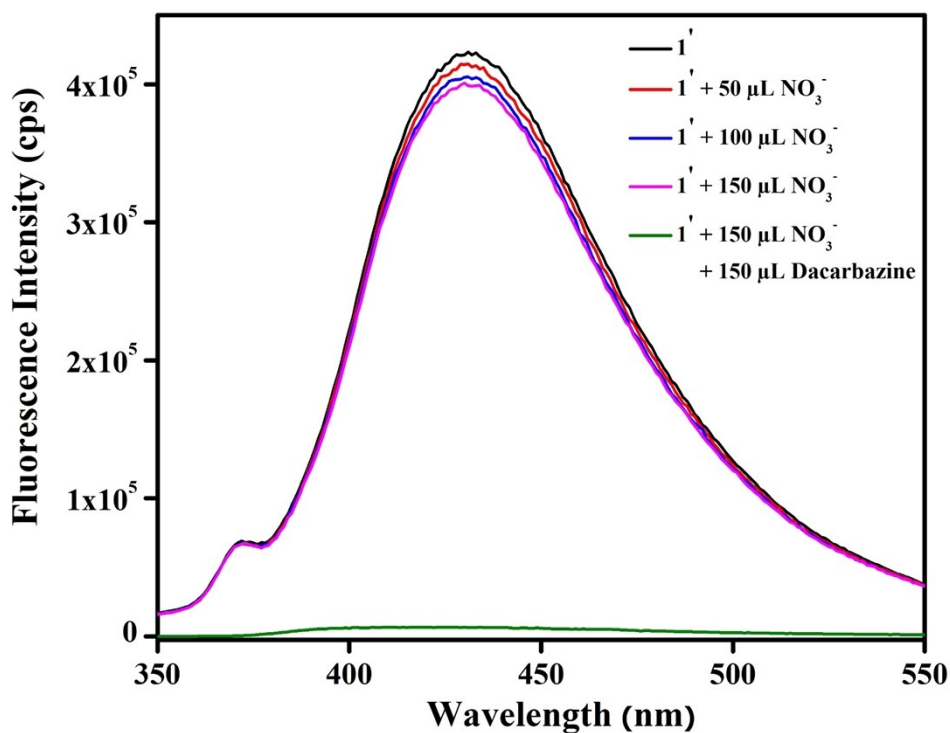


Figure S42. Quenching in fluorescence emission intensity of the suspension of 1' in HEPES buffer medium after addition of 150 μL of 10 mM (909 μM) dacarbazine solution in presence of 150 μL of 10 mM (476 μM) solution of NO_3^- .

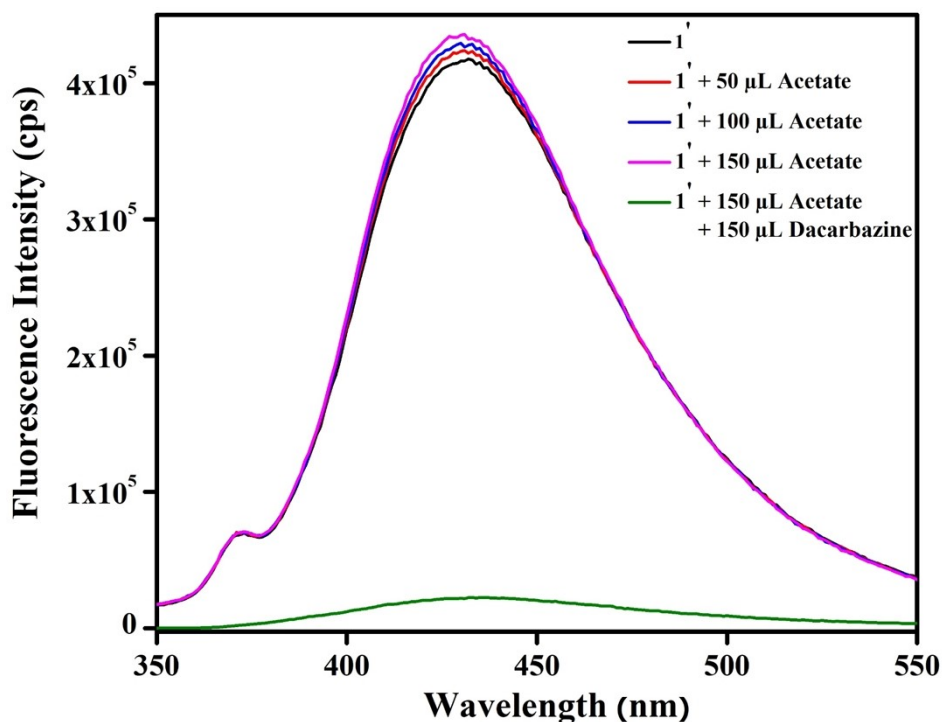


Figure S43. Quenching in fluorescence emission intensity of the suspension of 1' in HEPES buffer medium after addition of 150 μL of 10 mM (909 μM) DCZ solution in presence of 150 μL of 10 mM (476 μM) solution of acetate.

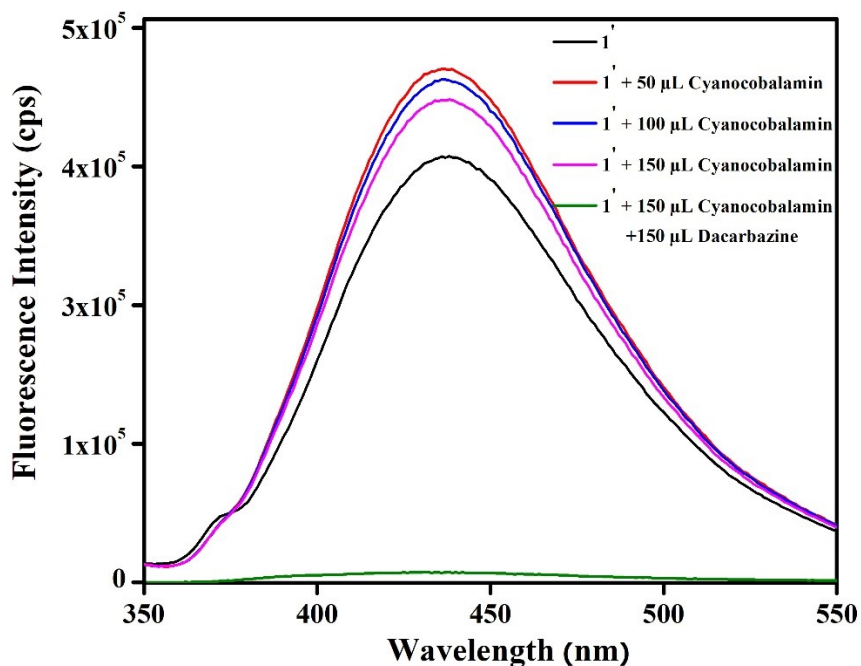


Figure S44. Quenching in fluorescence emission intensity of the suspension of **1'** in HEPES buffer medium after addition of 150 μL of 10 mM (909 μM) DCZ solution in presence of 150 μL of 10 mM (476 μM) solution of cyanocobalamin.

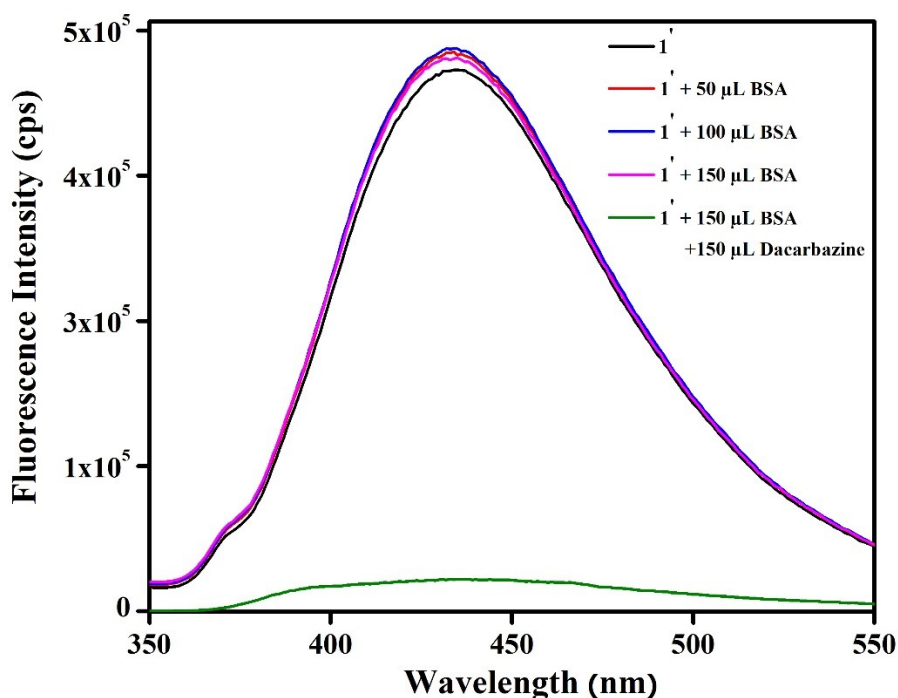


Figure S45. Quenching in fluorescence emission intensity of the suspension of **1'** in HEPES buffer medium after addition of 150 μL of 10 mM DCZ (909 μM) solution in presence of 150 μL of 10 mM (476 μM) solution of BSA.

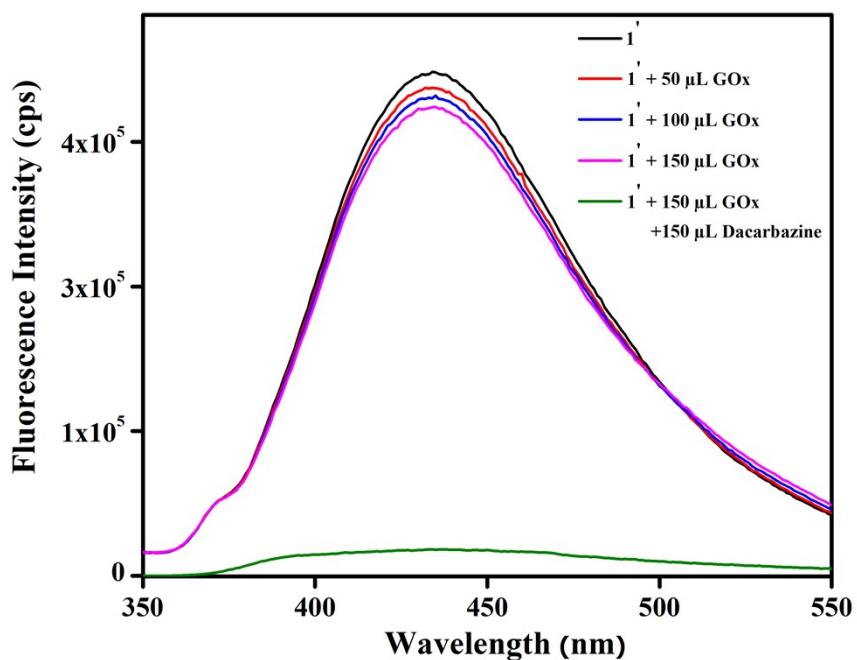


Figure S46. Quenching in fluorescence emission intensity of the suspension of **1'** in HEPES buffer medium after addition of 150 μL of 10 mM DCZ (909 μM) solution in presence of 150 μL of 10 mM (476 μM) solution of glucose oxidase (GOx).

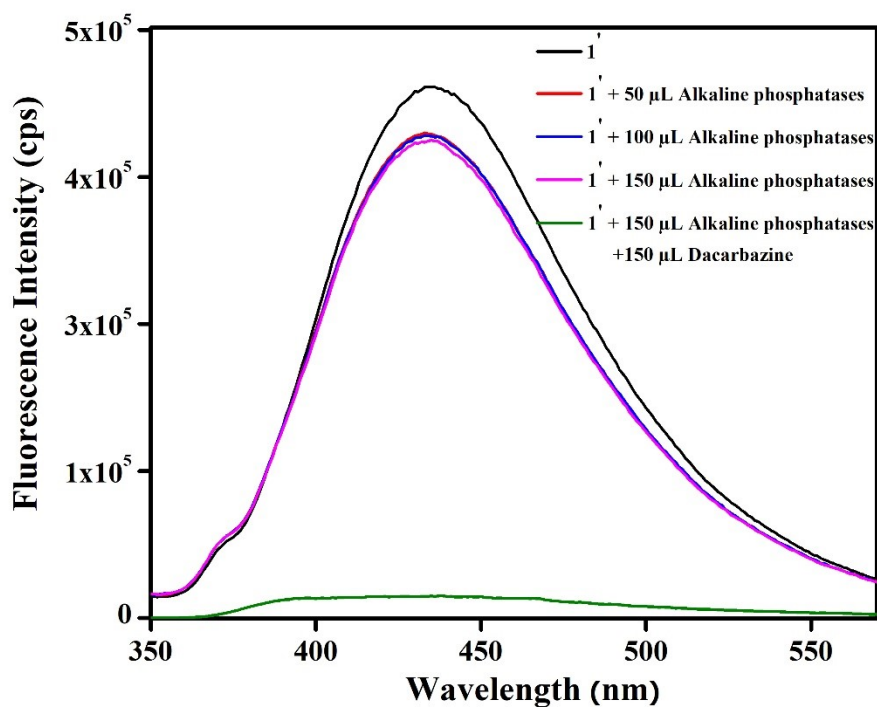


Figure S47. Quenching in fluorescence emission intensity of the suspension of **1'** in HEPES buffer medium after addition of 150 μL of 10 mM DCZ (909 μM) solution in presence of 150 μL of 10 mM (476 μM) solution of alkaline phosphatases.

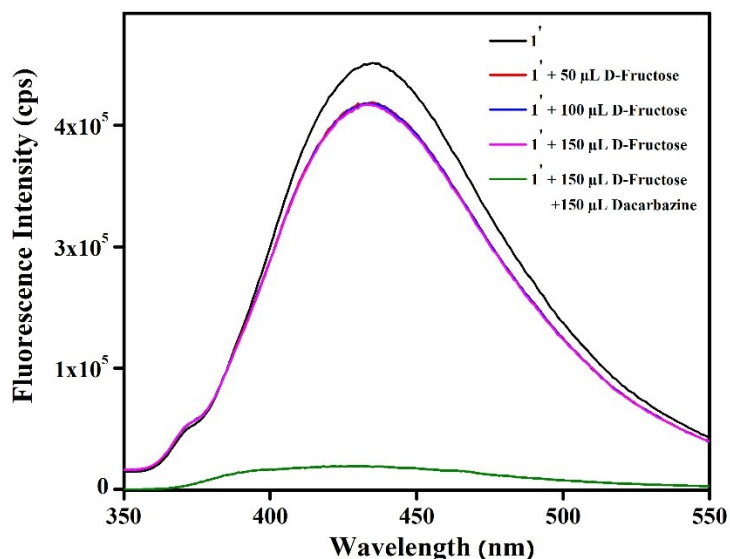


Figure S48. Quenching in fluorescence emission intensity of the suspension of 1' in HEPES buffer medium after addition of 150 μ L of 10 mM DCZ (909 μ M) solution in presence of 150 μ L of 10 mM (476 μ M) solution of D-fructose.

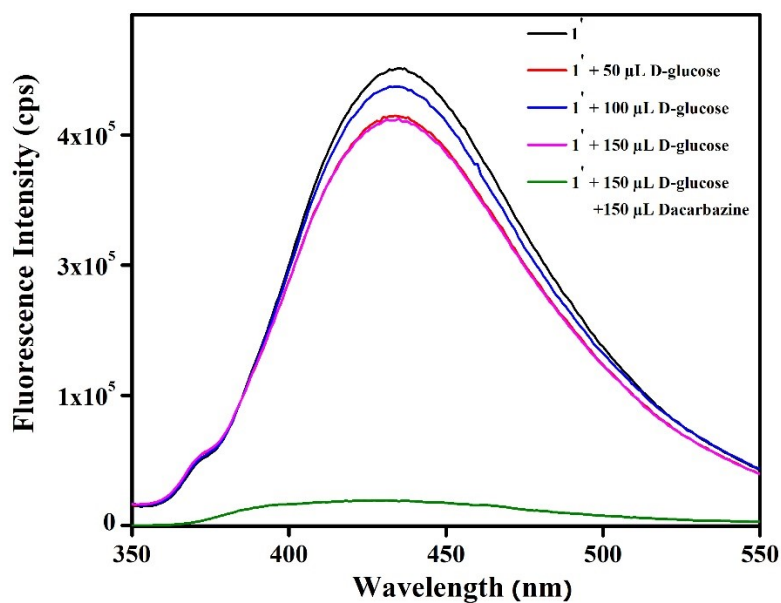


Figure S49. Quenching in fluorescence emission intensity of the suspension of 1' in HEPES buffer medium after addition of 150 μ L of 10 mM DCZ (909 μ M) solution in presence of 150 μ L of 10 mM (476 μ M) solution of D-glucose.

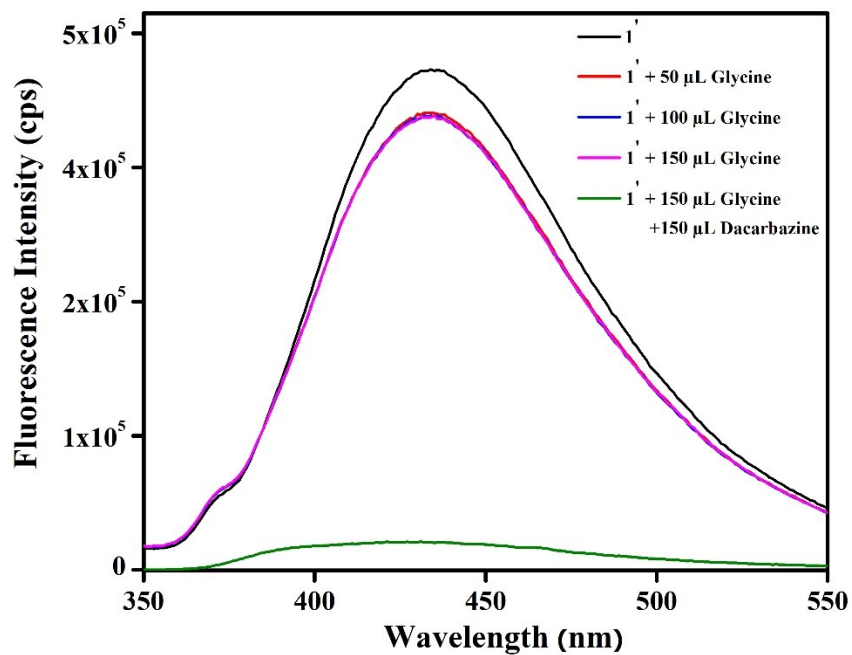


Figure S50. Quenching in fluorescence emission intensity of the suspension of **1'** in HEPES buffer medium after addition of 150 μ L of 10 mM (909 μ M) DCZ solution in presence of 150 μ L of 10 mM (476 μ M) solution of glycine.

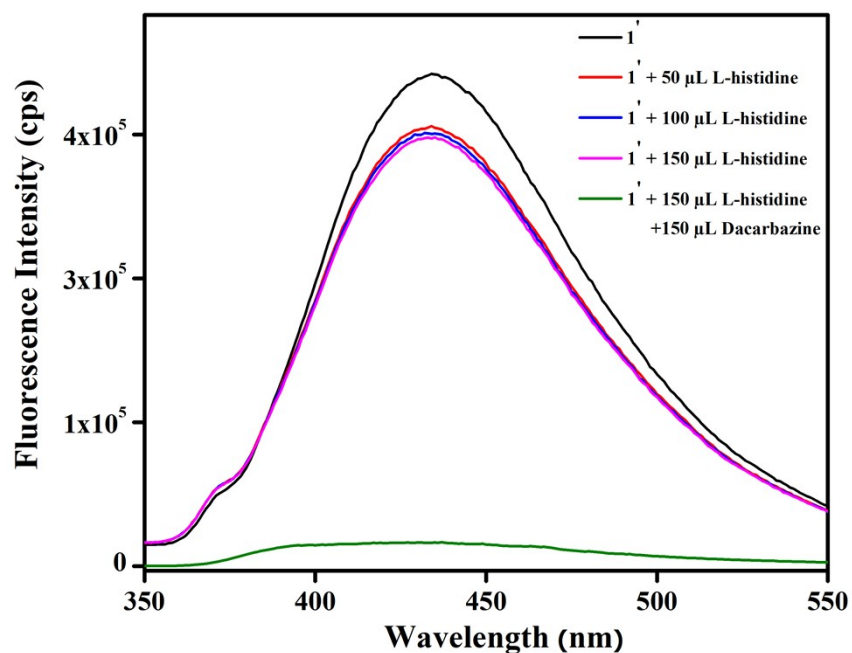


Figure S51. Quenching in fluorescence emission intensity of the suspension of **1'** in HEPES buffer medium after addition of 150 μ L of 10 mM (909 μ M) DCZ solution in presence of 150 μ L of 10 mM (476 μ M) solution of L-histidine.

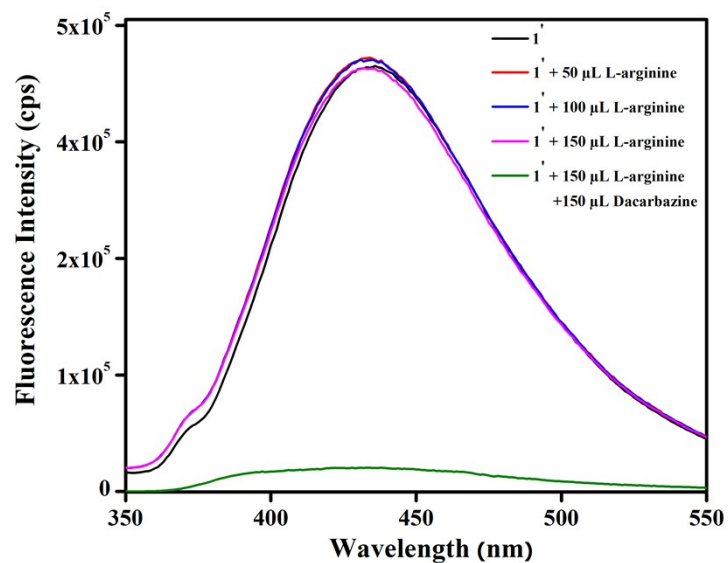


Figure S52. Quenching in fluorescence emission intensity of the suspension of **1'** in HEPES buffer medium after addition of 150 μL of 10 mM (909 μM) DCZ solution in presence of 150 μL of 10 mM (476 μM) solution of L-arginine.

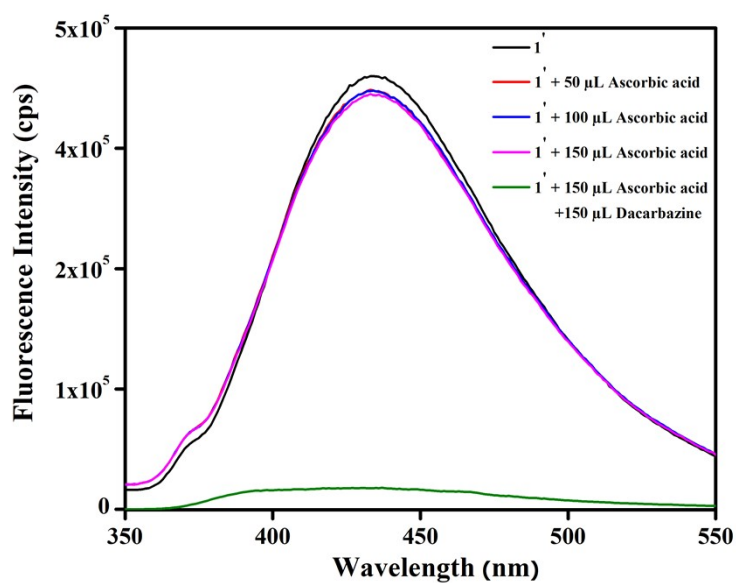


Figure S53. Quenching in fluorescence emission intensity of the suspension of **1'** in HEPES buffer medium after addition of 150 μL of 10 mM DCZ (909 μM) solution in presence of 150 μL of 10 mM (476 μM) solution of ascorbic acid.

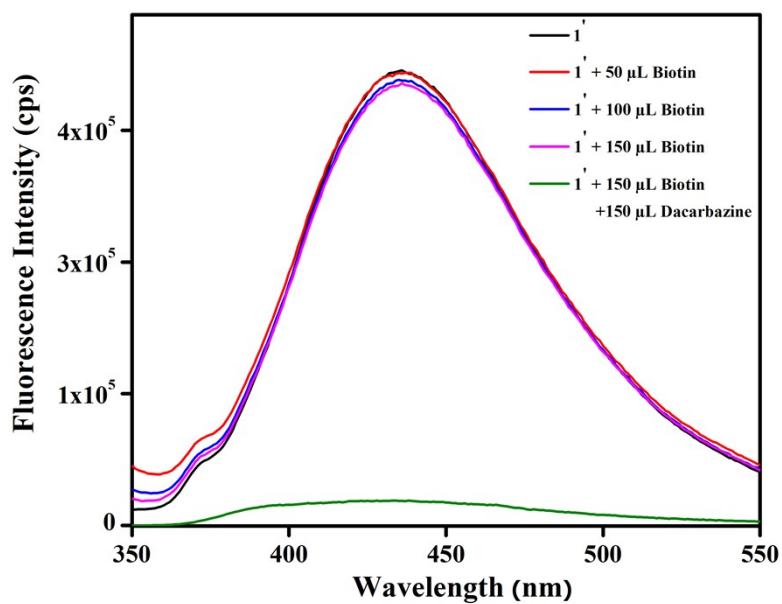


Figure S54. Quenching in fluorescence emission intensity of the suspension of **1'** in HEPES buffer medium after addition of 150 μL of 10 mM DCZ (909 μM) solution in presence of 150 μL of 10 mM (476 μM) solution of biotin.

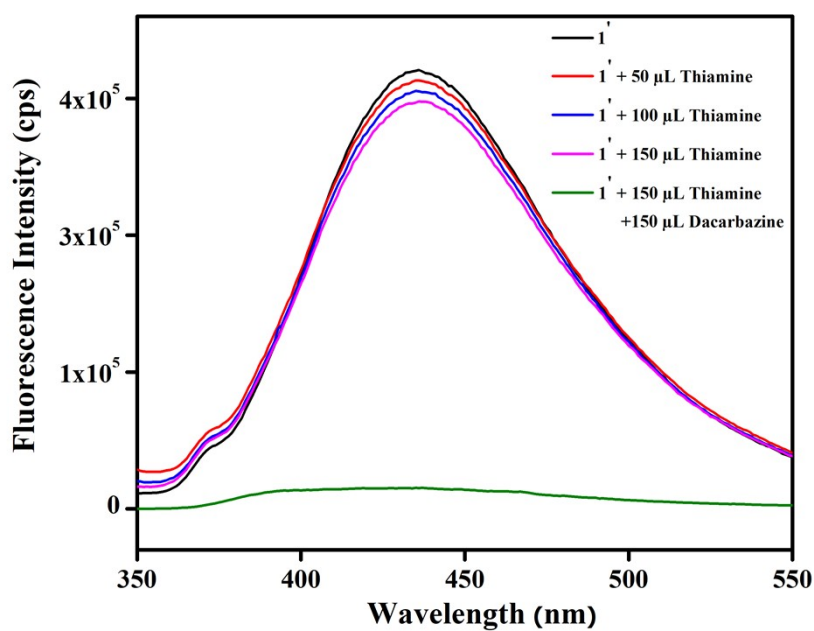


Figure S55. Quenching in fluorescence emission intensity of the suspension of **1'** in HEPES buffer medium after addition of 150 μL of 10 mM (909 μM) DCZ solution in presence of 150 μL of 10 mM (476 μM) solution of thiamine.

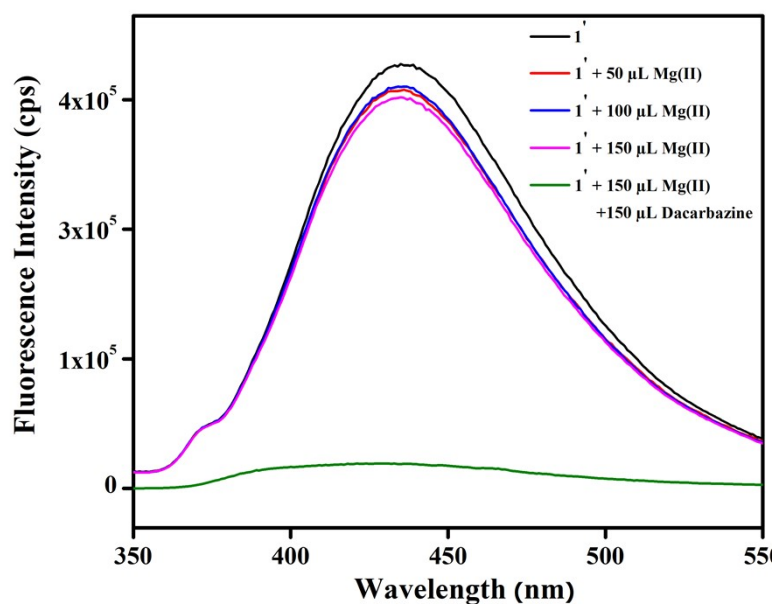


Figure S56. Quenching in fluorescence emission intensity of the suspension of **1'** in HEPES buffer medium after addition of 150 μL of 10 mM (909 μM) DCZ solution in presence of 150 μL of 10 mM (476 μM) solution of Mg(II).

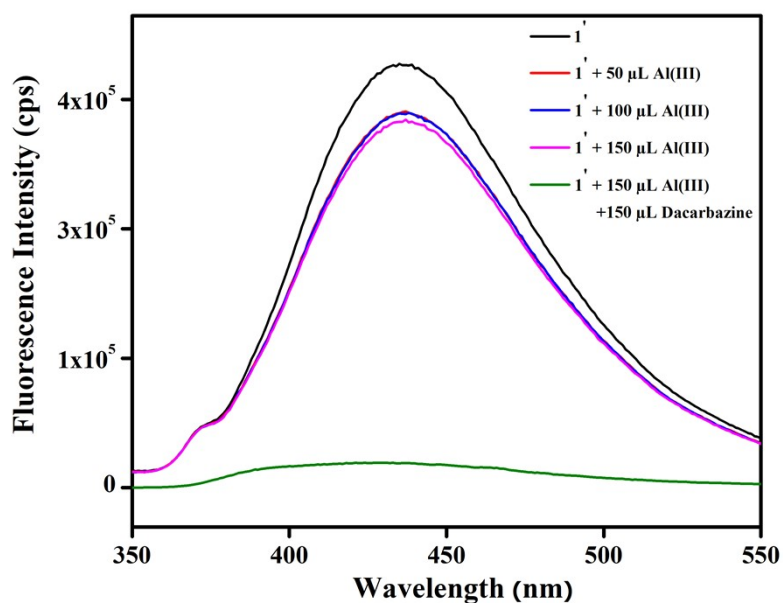


Figure S57. Quenching in fluorescence emission intensity of the suspension of **1'** in HEPES buffer medium after addition of 150 μL of 10 mM DCZ (909 μM) solution in presence of 150 μL of 10 mM (476 μM) solution of Al(III).

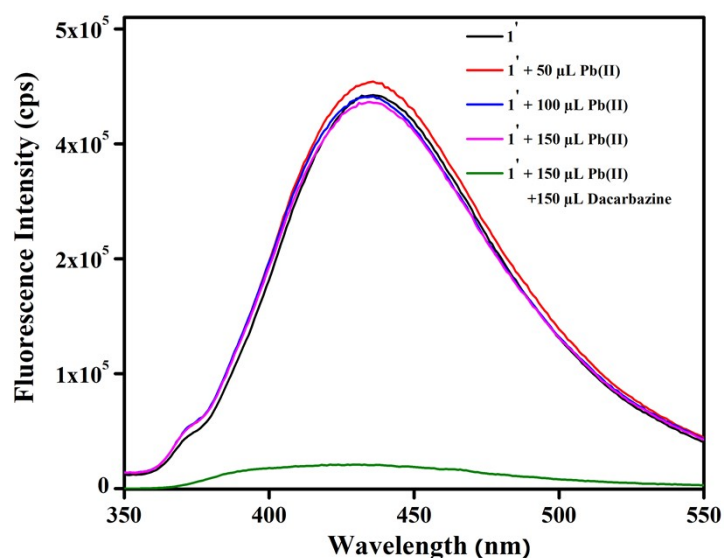


Figure S58. Quenching in fluorescence emission intensity of the suspension of **1'** in HEPES buffer medium after addition of 150 μL of 10 mM DCZ (909 μM) solution in presence of 150 μL of 10 mM (476 μM) solution of Pb(II).

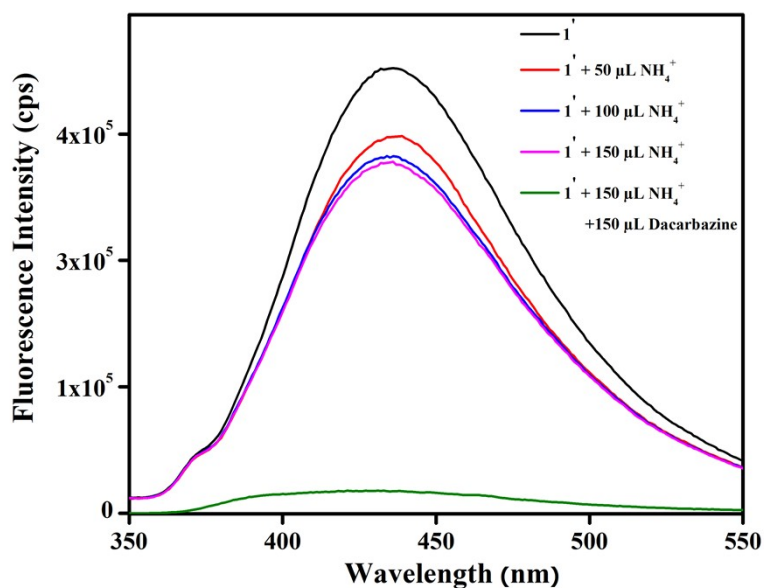


Figure S59. Quenching in fluorescence emission intensity of the suspension of **1'** in HEPES buffer medium after addition of 150 μL of 10 mM (909 μM) DCZ solution in presence of 150 μL of 10 mM (476 μM) solution of NH_4^+ .

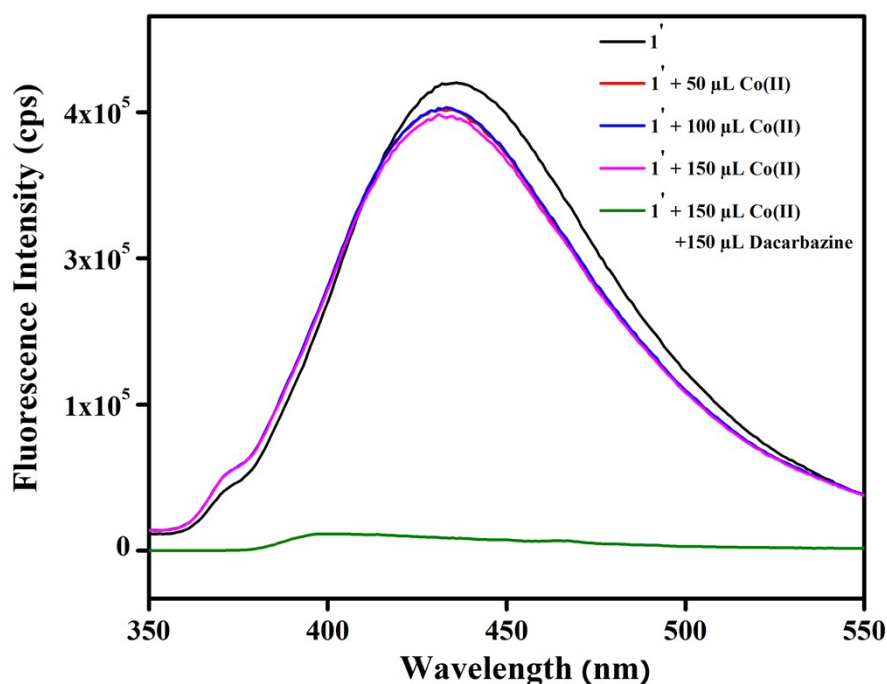


Figure S60. Quenching in fluorescence emission intensity of the suspension of **1'** in HEPES buffer medium after addition of 150 μL of 10 mM (909 μM) DCZ solution in presence of 150 μL of 10 mM (476 μM) solution of Co(II).

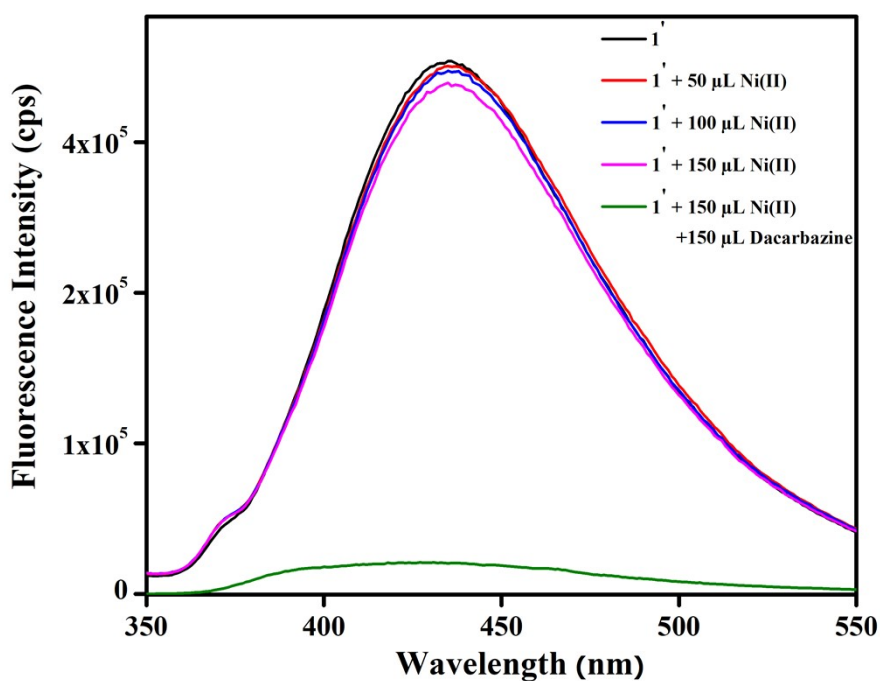


Figure S61. Quenching in fluorescence emission intensity of the suspension of **1'** in HEPES buffer medium after addition of 150 μL of 10 mM (909 μM) DCZ solution in presence of 150 μL of 10 mM (476 μM) solution of Ni(II).

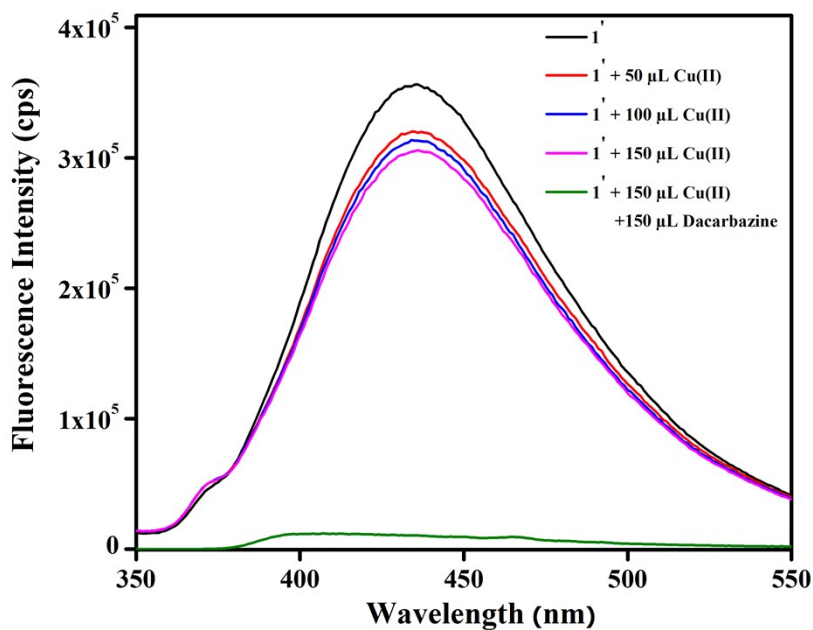


Figure S62. Quenching in fluorescence emission intensity of the suspension of **1'** in HEPES buffer medium after addition of 150 μL of 10 mM (909 μM) DCZ solution in presence of 150 μL of 10 mM (476 μM) solution of Cu(II).

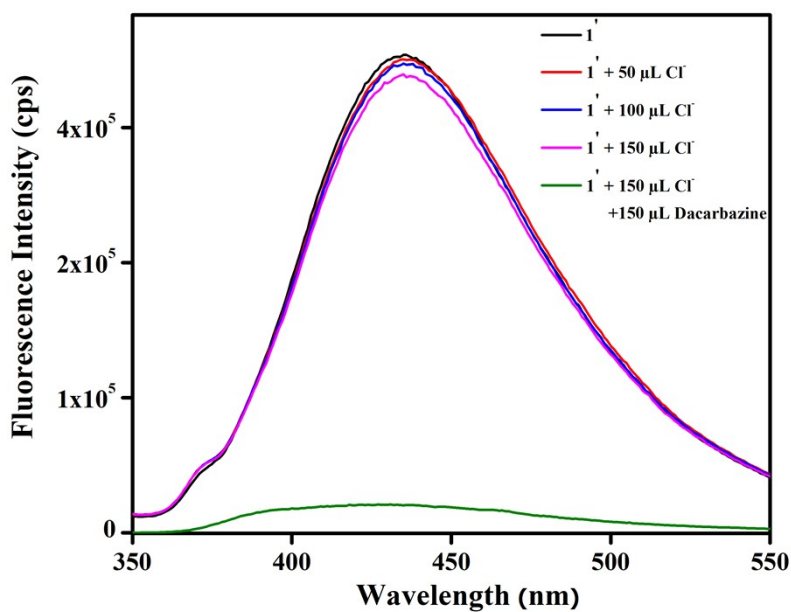


Figure S63. Quenching in fluorescence emission intensity of the suspension of **1'** in HEPES buffer medium after addition of 150 μL of 10 mM (909 μM) DCZ solution in presence of 150 μL of 10 mM (476 μM) solution of Cl⁻.

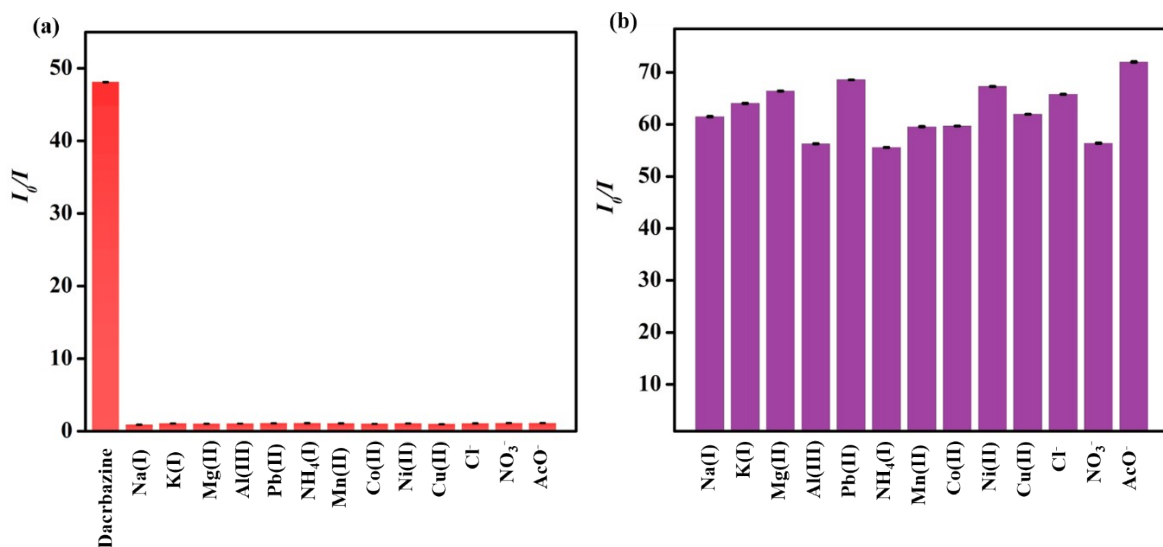


Figure S64. (a) Selective recognition of DCZ by 1' over other metal ions and anions. (b) Quenching efficiency of DCZ in the presence of other metal ions and anions.

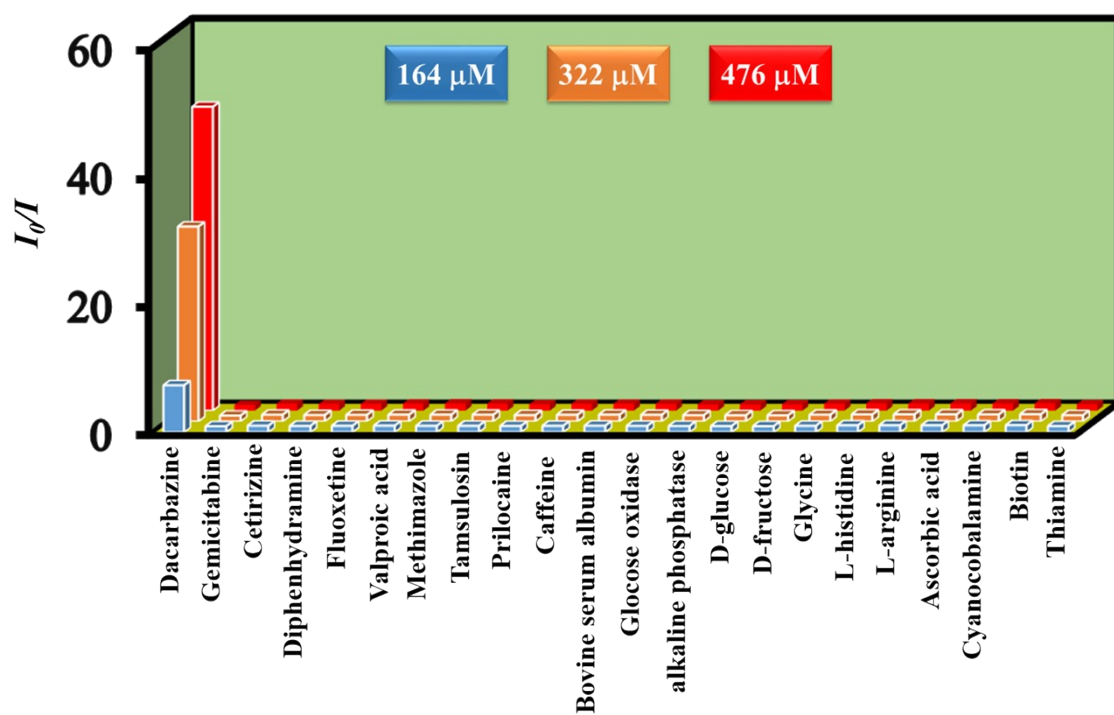


Figure S65. 3D Stern-Volmer plots for various analytes for DCZ sensing.

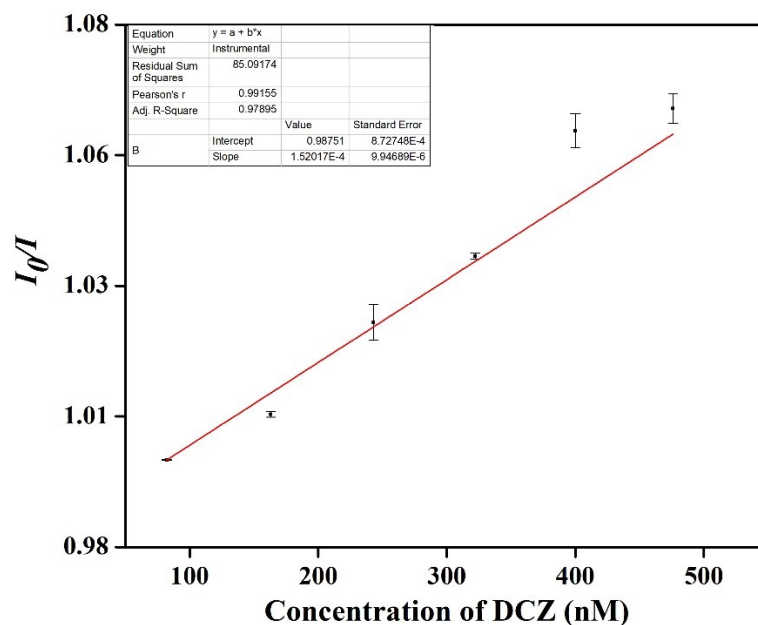


Figure S66. Stern-Volmer plot for the fluorescence emission quenching of **1'** in presence of DCZ.

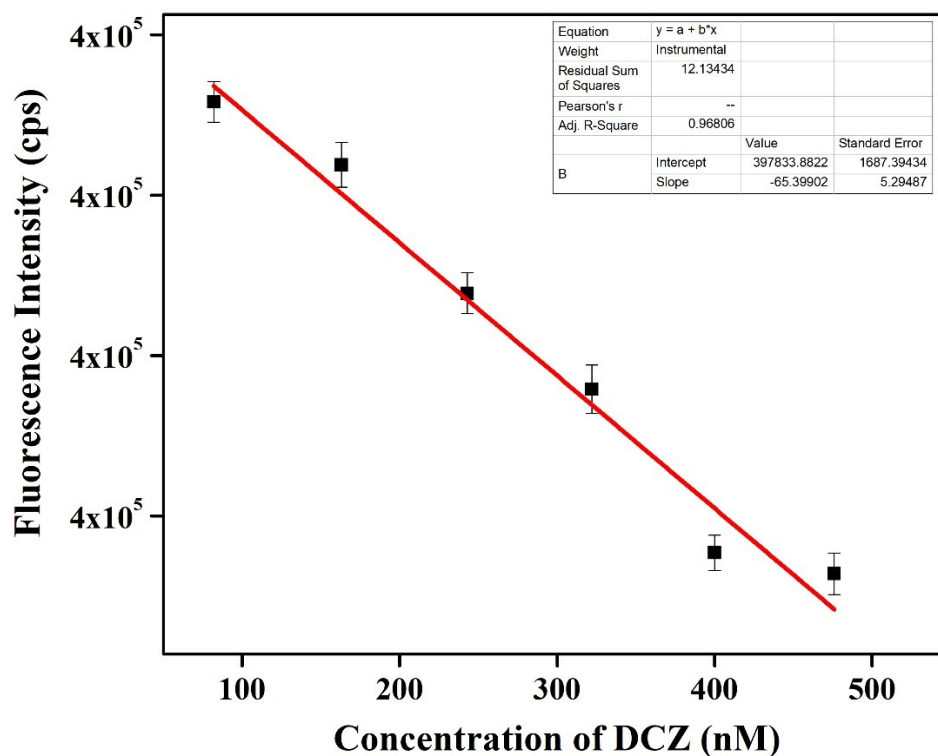


Figure S67. Change in the fluorescence emission intensity of **1'** as a function of concentration of dacarbazine.

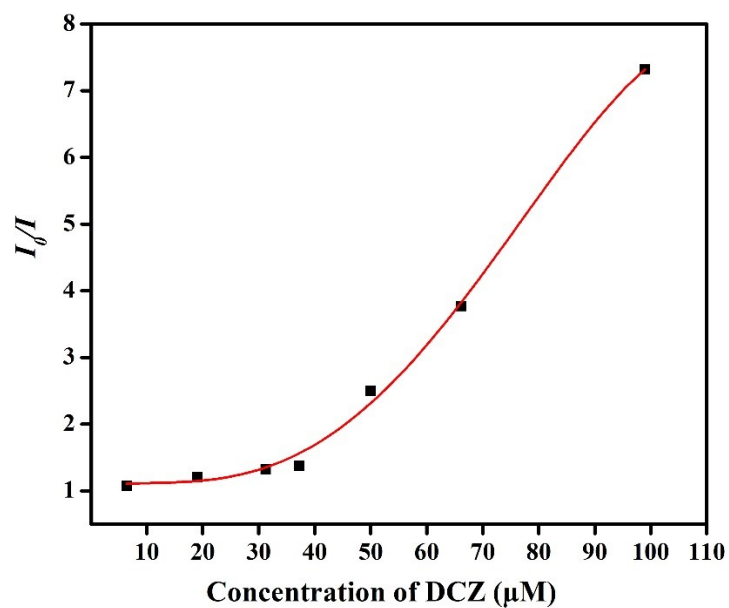


Figure S68. Stern-Volmer plot for fluorescence quenching of **1'** in HEPES buffer medium against increasing different concentrations of DCZ.

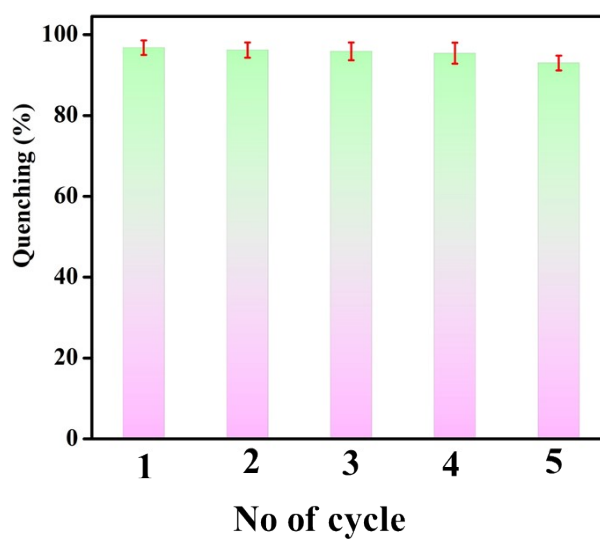


Figure S69. Recyclability test of probe **1'** for the sensing of 10 mM dacarbazine in aqueous medium.

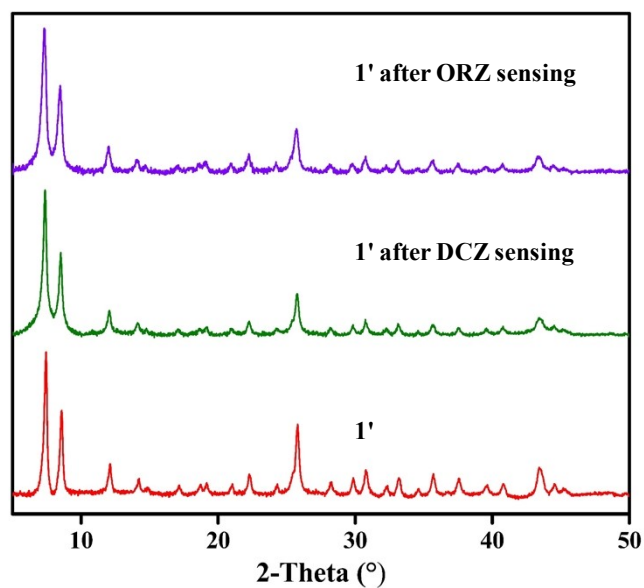


Figure S70. PXRD patterns of **1'** before and after sensing with DCZ and ORZ.

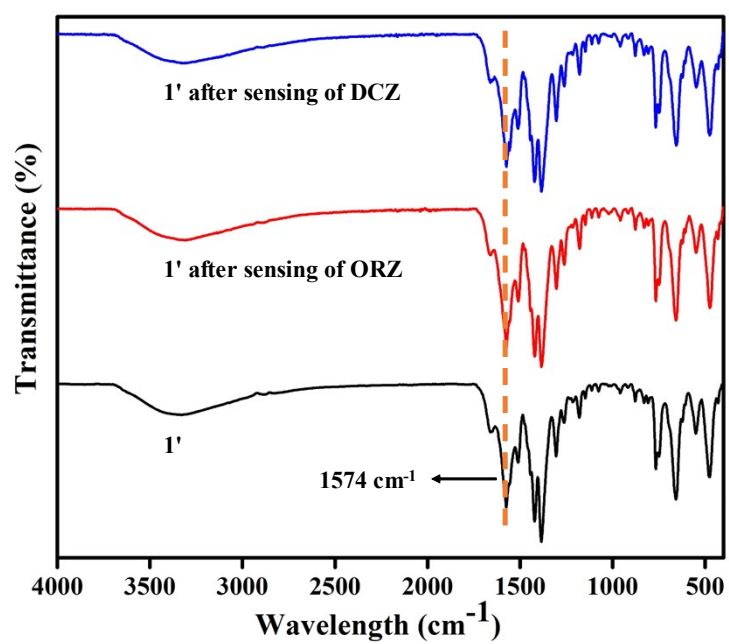


Figure S71. IR spectra of **1'** before and after sensing with ORZ and DCZ.

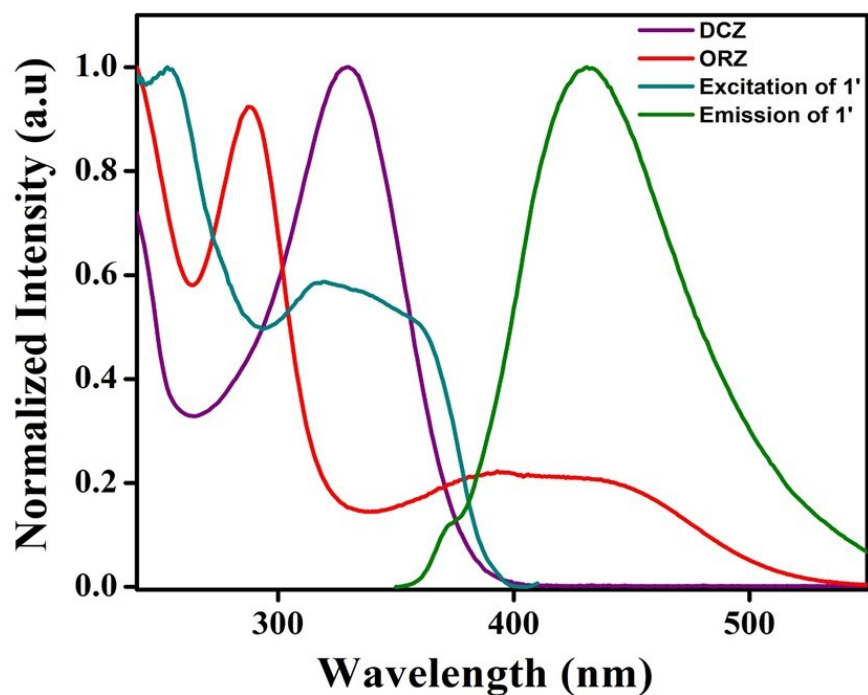


Figure S72. Overlap plot for UV-Vis spectra of competitive analytes of dacarbazine and oryzalin with the fluorescence excitation and emission spectra of 1'.

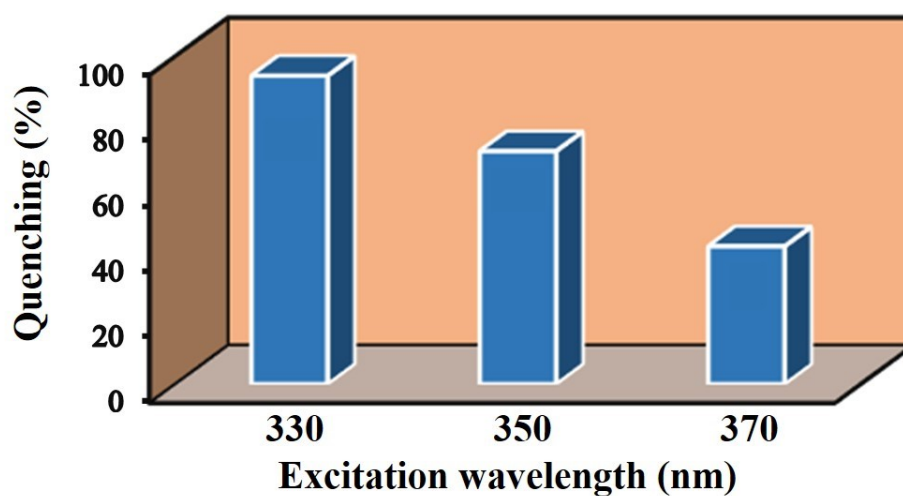
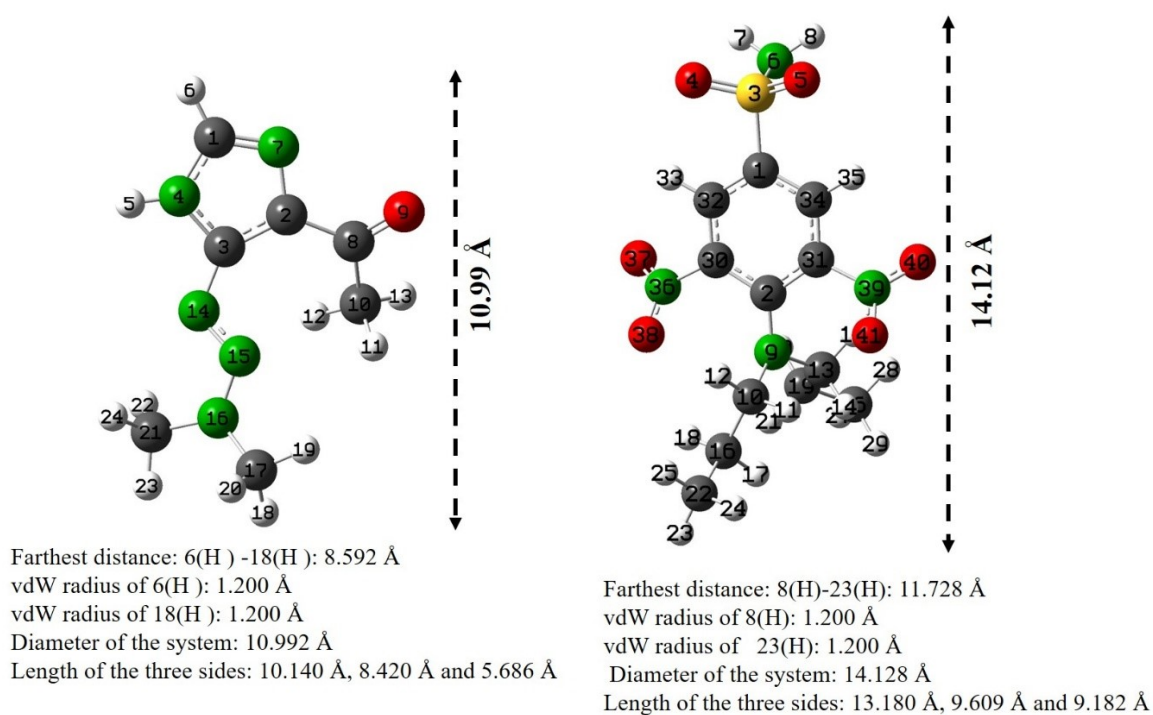


Figure S73. Quenching efficiency of 1' after addition of DCZ having different excited wavelength.

Table S2. Detection of DCZ in real samples.

Sample	Fluorometry Method			HPLC Method		
	DCZ Spiked (mol L ⁻¹)	DCZ Found (mol L ⁻¹)	Recovery (%)	DCZ Spiked (mol L ⁻¹)	DCZ Found (mol L ⁻¹)	Recovery (%)
Urine	1.27×10^{-5}	1.15×10^{-5}	90.5±4.6	2.43×10^{-5}	2.54×10^{-5}	104.5±0.7
Blood Serum	1.27×10^{-5}	1.21×10^{-5}	95.2±0.9	2.43×10^{-5}	2.50×10^{-5}	102.8±0.7



Scheme S2. Molecular size of (a) DCZ and (b) ORZ (C: dark grey, O: red, N: green, H: white) using DFT and Multifwn software.

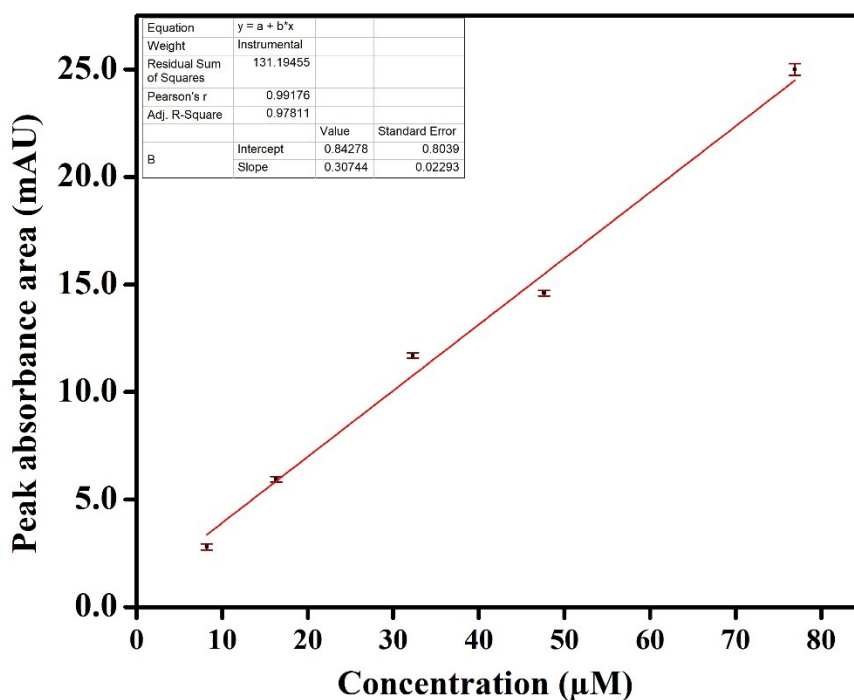


Figure S74. Calibration curve obtained from HPLC measurements for DCZ in water (absorption maxima was taken at 330 nm).

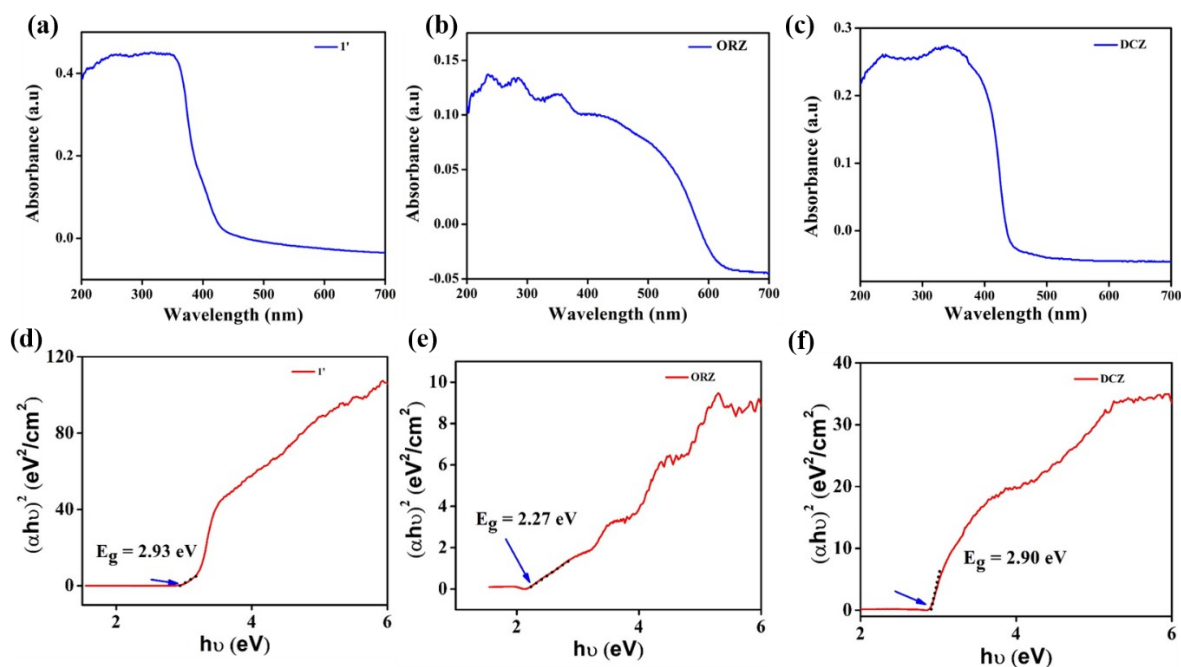


Figure S75. UV-DRS spectra of (a) **1'**, (b) ORZ and (c) DCZ. Tauc plots of (d) **1'**, (e) ORZ and (f) DCZ.

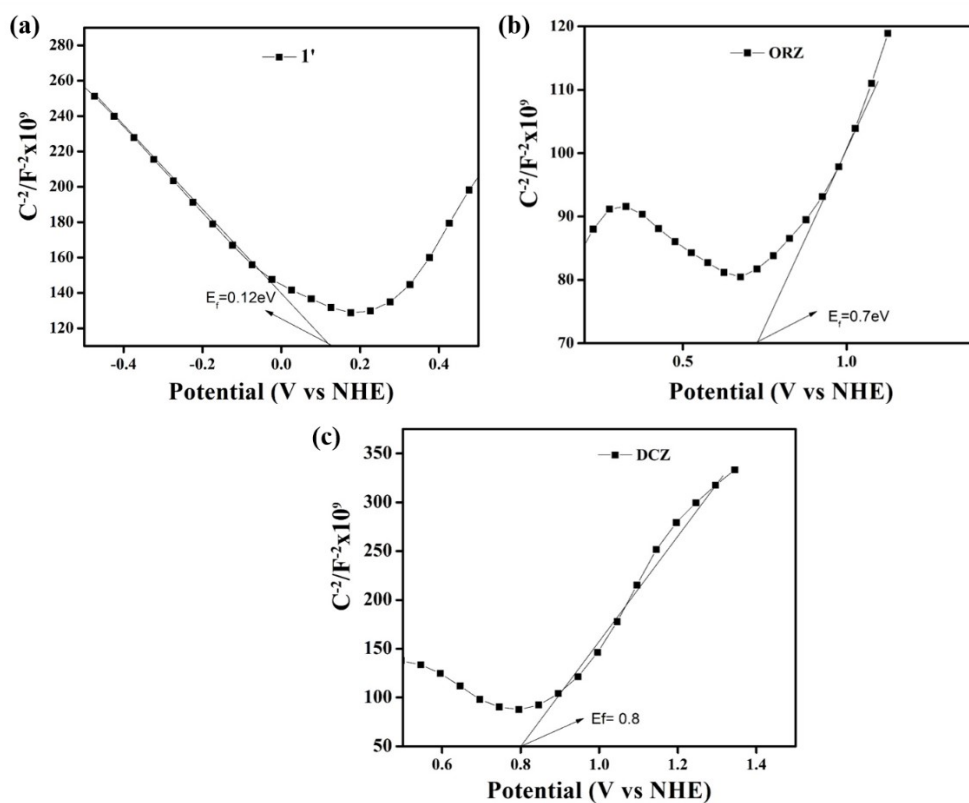
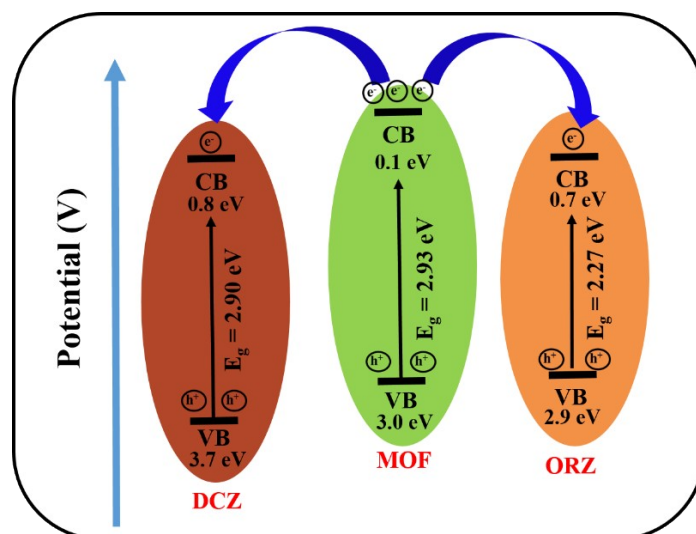


Figure S76. Mott-Schottky plots of (a) **1'**, (b) **ORZ** and (c) **DCZ**.



Scheme S3. Schematic representation of electron transfers from the CB of **1'** to the CB of **DCZ** and **ORZ** (CB = conduction band and VB = valence band).

References:

1. Cavka, J. H.; Jakobsen, S.; Olsbye, U.; Guillou, N.; Lamberti, C.; Bordiga, S.; Lillerud, K. P., A new zirconium inorganic building brick forming metal organic frameworks with exceptional stability. *J. Am. Chem. Soc.* **2008**, *130* (42), 13850-13851.